3-18-2019

Precision of Parameter Estimation in Quantum Metrology

Chenglong You
Louisiana State University and Agricultural and Mechanical College, yclong001@gmail.com

PRECISION OF PARAMETER ESTIMATION IN QUANTUM METROLOGY

A Dissertation

Submitted to the Graduate Faculty of the
Louisiana State University and
Agricultural and Mechanical College
in partial fulfillment of the
requirements for the degree of
Doctor of Philosophy

in

The Department of Physics & Astronomy

by
Chenglong You
B.S., Qingdao University, 2014
May 2019

Dedicated to my beloved grandparents.

Acknowledgments

I am greatly grateful to my advisor, Professor Jonathan P. Dowling. I still remember back in the days of my undergraduate life, when I was desperately trying to find a place for my Ph.D. study, he replied to my email within few hours, and detailed for me all potential weakness in my application and helped me through it. I am also thankful for all his support for my traveling and providing me with different opportunities throughout my study here. It is safe to say without his help, I could not be what I am now.

I am deeply grateful to my co-supervisor, Professor Georgios Veronis, whom I worked with on topics of photonics. His carefulness on every project and paper inspires me to work as rigorously as he does. He always listens to me and gives me great suggestions for my life and research.

I am also grateful to my friend and collaborator, Professor Omar Magaña-Loaiza. I thank him for helping me get into experiments in quantum optics. His way of thinking physics inspires me to continue to work in a similar field. I am also very grateful of him providing me a lot of opportunities on collaborating with talented physicists.

I also want to thank Professor Mark Wilde and Professor Hwang Lee from QST group. Prof.Wilde's classes on quantum information and quantum computation broaden my knowledge in quantum related research. Prof.Lee is always helpful and always friendly and open to discussions with me.

I am thankful to Professor Tim Byrnes at NYU Shanghai. Jon and Tim arranged the internship at NYU Shanghai, which I consider an excellent help for my future career. Prof. Byrnes is always open to new research topics, and he always tried his best to help me with my struggling in physics theory research.

I thank Dr.Masahiro Takeoka, who made my internship in Tokyo possible. He is accommodating since I had problems of language in Japan. He also provided me with a great research topic, and he helped a great ton on my papers and provided guidance. I also want to thank Dr.Tsujimoto Yoshiaki. You made my short stay in Tokyo fun and meaningful.

I will never forget the days we climbed Mt. Fuji and stayed for the hot-spring in Lake Kawaguchi.

I want to thank my friend, Dr.Sushovit Adhikari. We worked on homework together, we worked on research together, we went for an internship at Shanghai and Tokyo together. He always helps me without any hesitation, and I cannot thank him enough. I wish him a great career, and I hope we can again collaborate in the near future.

I am grateful to Dr.Jonathan Olson and Dr.Bryan Gard, who introduced me into the research of quantum optics. I also want to thank Christopher Granier and Simon Lorenzo, who became close friends with me after I joined QST. I want to thank Dr.Haoyu Qi and Dr.Xiaoping Ma, who are my best Chinese friends, to talk about research and giving me help all the time. I also thank my all friends from QST group, your presence brings wonderfulness in my Ph.D. study.

I also want to thank my internet friends, whom I talked to frequently about almost everything including gaming, personal life, and even research. With you guys, my life is much more wonderful and fun.

I want to thank my family for supporting me throughout my study here. Without them, I could not have the opportunity to be here in the first place. I want to thank my wife Chuqi Guo, for taking care of my life and always be there when I need her the most.

Lastly, I would like to acknowledge financial support from Economic Development Assistantship from Louisiana State University System Board of Regents. I would also like to acknowledge support National Science Foundation (NSF) without which the work in this dissertation would not have been possible.

Table of Contents

List of Figures

Abstract

The fundamental precision limit of an interferometer is crucial since it bounds the best possible sensitivity one could achieve using such a device. This thesis will focus on several different interferometers and try to give the ultimate precision bounds by carefully counting all the resources used in the interferometers.

The thesis begins with the basics of the quantum state of light. The fundamentals of quantum metrology are also reviewed and discussed. More specifically, the terminology of classical and quantum Cramér-Rao bound and classical and quantum Fisher information are introduced.

Chapter 3 discusses the conclusive precision bounds in two-mode interferometer such as Mach-Zehnder interferometer (MZI) and SU(1,1) interferometer. I revisit the quantum Fisher information approach of these two interferometers and show the discrepancy of phase sensitivity on the physically same setup. Then I establish fundamental precision estimation bounds for such device, due to the reason that many works of literature fail to accurately count the resources and knowledge of phase-to-be-estimated used in the interferometers. The analysis suggests that for a MZI, one can never do better than SNL in phase sensitivity, when an input to one of the two ports is the vacuum. If one does not allow the detector to use any external phase reference or power resource, then the precision is limited by the SNL. For a SU(1,1) interferometer, firstly, when one of the input states is restricted to be a vacuum state, I showed that by using either the phase-averaging method or the quantum Fisher information matrix method, different phase configurations of the SU(1,1) interferometer result in the same QFI. Secondly, I compared the results of the phase-averaging method and the quantum Fisher information matrix method, and then I argued that for an SU(1,1) interferometer, phase averaging or quantum Fisher information matrix method is generally required, and they are equivalent. Finally, I used the quantum Fisher information matrix method to calculate the precision limit for other common input states, such as two coherent state inputs or coherent state with squeezed vacuum inputs.

In chapter 4, I will consider a passive multi-mode interferometer for multiparameter phase estimation. It was suggested that optical networks with relatively inexpensive overhead—single photon Fock states, passive optical elements, and single photon detection—can show significant improvements over classical strategies for single-parameter estimation, when the number of modes in the network is small. In this chapter, I analytically compute the quantum Cramér-Rao bound to show these networks can have a constant-factor quantum advantage in multi-parameter estimation for even large number of modes. Additionally, I provide a simplified measurement scheme using an array of single photon detectors and only one number-resolving detector that is capable of approximately obtaining this sensitivity for a small number of modes. Remarkably, supersensitivity can be observed even with inefficient but heralded single photon sources.

Chapter 1
Introduction

The discovery of quantum mechanics enables us to further explore the properties of objects in a much smaller scale. Classical metrology considers the accuracy of the estimation, which is typically limited. The most fundamental setup of metrology is a two-mode Mach-Zehnder (MZ) interferometer, which has an unknown phase difference between its two arms. The goal is to estimate this phase with high precision, which could lead to great interest in a variety of fields such as quantum laser radar (LADAR) [1, 2], quantum lithography [3, 4], and gravitational wave detection [5, 6].

When considering the whole metrology setup using semi-classical theory, i.e., we treat light using classical theory while treat the detection scheme by quantum theory, the uncertainty of the measurement typically is bounded by *shotnoise*, which is given by $\Delta\varphi = 1/\sqrt{\bar{n}}$, where $\bar{n}$ is the average photon number of the resource used in the interferometer. For a long time, shotnoise was considered to be the ultimate limit of any metrology device. However, when considering metrology technology using quantum theory as a whole, one can achieve better estimation precision than shotnoise [7].

For example, by using laser light in one arm, and vacuum in the other arm of the MZI, together with intensity detection, one gets back the shotnoise limit (SNL), which is given by $1/\sqrt{n_\alpha}$, where n_α is the average photon number of the laser light. However, by utilizing quantum states and quantum detection schemes, it has been shown that one can beat the shotnoise and achieve better sensitivity, or even the Heisenberg limit (HL), which is given by $\Delta\varphi = 1/\bar{n}$.

Typically, the sensitivity of the metrology setup is determined by the input state, the interaction of the phase and input state, as well as the detection method. For instance, in 1981, Caves showed that by using non-classical states of light such as squeezed vacuum [8], one could beat the SNL. Later, different states such as N00N states [9], twin Fock states [10] and two-mode squeezed states [11] were shown to be useful when one tries to beat SNL

and even achieve Heisenberg sensitivity.

The other way to beat SNL is to use active elements in an interferometer. One such interferometer is called a SU(1,1) interferometer, introduced by Yurke et al. in 1986 [12], where the beam splitters in the MZI are replaced by an active element, such as an optical parametric amplifier (OPA) or four-wave mixer, which are mathematically characterized by the group SU(1,1). These interferometers can achieve Heisenberg sensitivity even if inputs are both vacua. Since first proposed, the phase sensitivity of the SU(1,1) interferometer has been extensively studied both in theory and experiment.

To calculate the estimation precision of the interferometer, one can use the error propagation formula for a given measurement scheme [13]. However, to find the best possible estimator for the given system, one needs to exhaust all possible measurement strategies, which renders the problem nearly impossible to solve. However, with the help of quantum Fisher information (QFI) [14], one could find the ultimate precision bounds of the phase sensitivity without determining a measurement. Then the sensitivity is given by the quantum Cramér-Rao (QCRB) bound [14, 15], $\Delta^2\phi \geq 1/F_Q$, where F_Q is the QFI.

This thesis is structured as follows: In Chapter 2, I will discuss the different quantum states of light along with their application in a Mach-Zehnder interferometer. The fundamentals of quantum metrology are also reviewed and discussed. I will also introduce the terminology of classical and quantum Cramér-Rao bound and classical and quantum Fisher information. In Chapter 3, I will revisit the QFI approach to the calculation of the precision of the parameter estimation in Mach-Zehnder interferometer and SU(1,1) interferometer. Then I will show that by utilizing phase-randomizing or quantum Fisher information approach, one can bound the precision of parameter estimation tighter for SU(1,1) interferometer, and recover the no-go theorem for MZI. In Chapter 4, I will consider a passive multi-mode interferometer for multiparameter phase estimation. I will analytically compute the quantum Cramér-Rao bound to show these networks can have a constant-factor quantum advantage in multi-parameter estimation for even large number of modes.

Additionally, I will provide a simplified measurement scheme using an array of single photon detectors and only one number-resolving detector that is capable of approximately obtaining this sensitivity for a small number of modes.

Chapter 2
Preliminaries of Quantum Optics and Quantum Metrology

2.1 Introduction

In this chapter, I will review the basics of quantum optics such as quantum states of light. Later I will also discuss the fundamentals of quantum metrology.

2.2 Quantization of Electromagnetic Field

To quantize the electromagnetic field of light, one can first start with the quantization of the classical electromagnetic field equation of motion, namely Maxwell's equations. Assuming that there are no sources of radiation, thus the Maxwell equations become,

$$\nabla \times \vec{E} = -\frac{\partial \vec{B}}{\partial t}, \tag{2.1}$$

$$\nabla \times \vec{B} = \frac{1}{c^2}\frac{\partial \vec{E}}{\partial t}, \tag{2.2}$$

$$\nabla \cdot \vec{B} = 0, \tag{2.3}$$

$$\nabla \cdot \vec{E} = 0, \tag{2.4}$$

where $\vec{B} = \mu_0 \vec{H}$ and $\vec{D} = \varepsilon_0 \vec{E}$. Here $\vec{E}$ and $\vec{B}$ represent electric and magnetic field, respectively, while μ_0 and ε_0 represent the magnetic permeability and dielectric permittivity of free space, respectively. In addition, $\mu_0 \varepsilon_0 = 1/c^2$, where c is the speed of light in free space.

Then by introducing the magnetic potential $\vec{A}$ and electric potential $V(\vec{r})$, one obtains

$$\vec{B} = \nabla \times \vec{A}, \tag{2.5}$$

$$\vec{E} = -\frac{\partial \vec{A}}{\partial t} - \nabla V(\vec{r}). \tag{2.6}$$

Combining these two equations, one gets

$$\nabla^2 \vec{A} = \frac{1}{c^2} \frac{\partial^2 \vec{A}}{\partial t^2}. \tag{2.7}$$

The above equation is Maxwell's wave equation under the Coulomb Gauge condition in free space. Then considering a one-dimensional cavity with length L, with the radiation field's direction of propagation along the z direction and polarized along the x direction, one obtain the single-mode field,

$$E_x(z,t) = \sum_l A_l Q_l(t) \sin(k_l z), \tag{2.8}$$

where k_l and Q_l are the wave number and amplitude of the lth mode, respectively, and $A_l = \sqrt{2\omega_l^2/(V\varepsilon_0)}$. Since the one-dimensional boundary condition must be met, $k_l = j\pi/L \quad (l = 1, 2, 3, \cdots)$. Then the magnetic field in the cavity, following Maxwell's equation, is

$$B_y(z,t) = \frac{1}{c^2} \sum_l A_l \frac{\dot{Q}(t)}{k_l} \cos(k_l z). \tag{2.9}$$

Then the classical field energy of the single-mode field, i.e, the Hamiltonian H, is given by

$$H = \frac{1}{2} \int_v (\mu_0 \vec{H} + \varepsilon_0 \vec{E}^2) dV = \sum_l \frac{1}{2} (p_l^2 + \omega_l^2 q_l^2), \tag{2.10}$$

where $p_l = \dot{q}_l$. Then it is clear that the single-mode field is equivalent to a harmonic oscillator of unit mass. In this sense, one can get the Hamiltonian of the l_{th} harmonic oscillator as

$$\frac{dp_l}{dt} = -\frac{\partial H_l}{\partial q_l} = -\omega_l^2 q_l \tag{2.11}$$

$$\frac{dq_l}{dt} = \frac{\partial H_l}{\partial p_l} = p_l, \tag{2.12}$$

where

$$H_l = \frac{1}{2}(p_l^2 + \omega_l^2 q_l^2). \tag{2.13}$$

In order to quantize the single-mode field, one can then introduce the canonical commutation relation,

$$[\hat{q}_i, \hat{p_j}] = i\hbar\delta_{ij}, \tag{2.14}$$

where $\hbar = h/2\pi$. Then by convention, let us introduce the annihilation $\hat{a}_l$ and creation $\hat{a}_l^\dagger$ operators defined as

$$\hat{a}_l = \sqrt{\frac{1}{2\hbar\omega_l}}(\omega_l \hat{q}_l + i\hat{p}_l), \tag{2.15}$$

$$\hat{a}_l^\dagger = \sqrt{\frac{1}{2\hbar\omega_l}}(\omega_l \hat{q}_l - i\hat{p}_l). \tag{2.16}$$

The annihilation operator $\hat{a}_l$ and creation operator $\hat{a}_l^\dagger$ satisfy the commutation relation

$$\left[\hat{a}_j, \hat{a}_i^\dagger\right] = \delta_{ij}. \tag{2.17}$$

Therefore, the Hamiltonian can be written as

$$\hat{H} = \sum_l \hbar\omega_l(\hat{a}_l^\dagger \hat{a}_l + \frac{1}{2}). \tag{2.18}$$

Thus, one successfully quantized the electromagnetic field.

2.2.1 Fock States

In the last section, I reviewed the quantization of the electromagnetic field and introduced the annihilation operator $\hat{a}$, creation operator $\hat{a}^\dagger$, and Hamiltonian $\hat{H}$. Let me now introduce the Fock states, the eigenstates of Hamiltonian $\hat{H}$, and denote them as $|n\rangle$. One particular property of the Fock state is that it has a well-defined number of particles. Accordingly, let us define the particle number operator $\hat{N} = \hat{a}^\dagger\hat{a}$ which satisfies

$$\hat{N}\,|n\rangle = n\,|n\rangle\,. \tag{2.19}$$

The action of the creation and annihilation operators on the Fock state $|n\rangle$ is given by

$$\hat{a}^\dagger|n\rangle = \sqrt{n+1}|n+1\rangle, \tag{2.20}$$

$$\hat{a}|n\rangle = \sqrt{n}|n-1\rangle. \tag{2.21}$$

In addition, the number state $|n\rangle$ can be obtained from the vacuum state $|0\rangle$ as

$$|n\rangle = \frac{(\hat{a}^\dagger)^n}{\sqrt{n!}}|0\rangle. \tag{2.22}$$

From the equation above, one can also derive some properties of the Fock state. First, the Fock state is orthonormal:

$$\langle n|m\rangle = \delta_{nm}, \tag{2.23}$$

and the Fock state basis is complete:

$$\sum_{n=0}^{\infty} |n\rangle \langle n| = \hat{I}. \tag{2.24}$$

2.2.2 Coherent States

In this section, I will introduce another common field, which is called coherent state. The coherent states are based on the coherence quantum theory, and they represent the theoretical model of a laser. The definition of a coherent state is given by the annihilation operator

$$\hat{a}\,|\alpha\rangle = \alpha\,|\alpha\rangle\,. \tag{2.25}$$

Therefore, one can see that the coherent state is an eigenstate of the annihilation operator. Since the Fock state is a complete basis, one can represent coherent state in Fock state basis as

$$|\alpha\rangle = \exp\left(-\frac{1}{2}|\alpha|^2\right) \sum_{n=0}^{\infty} \frac{\alpha^n}{\sqrt{n!}}\,|n\rangle\,. \tag{2.26}$$

One can see that coherent states do not have a definite photon number, and, if the photon number is measured, its distribution follows the Poisson statistics,

$$P(n) = e^{-|\alpha|^2} \frac{|\alpha|^{2n}}{n!}, \tag{2.27}$$

with standard deviation of $\Delta n = |\alpha| = \sqrt{\langle n \rangle}$. The average photon number of the coherent state is

$$\left\langle \hat{N} \right\rangle = \langle \alpha | \, \hat{a}^\dagger \hat{a} \, | \alpha \rangle = |\alpha|^2. \tag{2.28}$$

In addition, the coherent states can be generated by displacing the vacuum state $|0\rangle$ with a displacement operator $\hat{D}(\alpha)$ as

$$|\alpha\rangle = \hat{D}(\alpha)|0\rangle, \tag{2.29}$$

where the displacement operator $\hat{D}(\alpha)$ is defined as $\hat{D}(\alpha) = \exp(\alpha \hat{a}^\dagger - \alpha^* \hat{a})$.

The coherent state has the following properties: First, the coherent state is non-orthogonal:

$$\langle \alpha | \, \beta \rangle = \exp(-\frac{1}{2}|\alpha|^2 - \frac{1}{2}|\beta|^2 + \alpha^* \beta). \tag{2.30}$$

Second, the coherent state is over-complete:

$$\frac{1}{\pi} \int |\alpha\rangle \, \langle \alpha | d^2\alpha = \hat{I}. \tag{2.31}$$

Third, the coherent state is a minimum uncertainty state and has equal uncertainties in both $\hat{X}_1$ and $\hat{X}_2$ quadratures, where the two Hermitian quadrature operators $\hat{X}_1$ and $\hat{X}_2$ are defined as

$$\hat{X}_1 = \frac{\hat{a} + \hat{a}^\dagger}{2}, \tag{2.32}$$

$$\hat{X}_2 = \frac{\hat{a} - \hat{a}^\dagger}{2i}. \tag{2.33}$$

They satisfy the following commutation and Heisenberg uncertainty relations:

$$[\hat{X}_1, \hat{X}_2] = \frac{i}{2}, \qquad \langle(\Delta\hat{X}_1)^2\rangle\langle(\Delta\hat{X}_2)^2\rangle \geq \frac{1}{16}. \tag{2.34}$$

For a coherent state one have

$$\left\langle \hat{X}_1 \right\rangle = \mathrm{Re}(\alpha), \tag{2.35}$$

$$\left\langle \hat{X}_2 \right\rangle = \mathrm{Im}(\alpha), \tag{2.36}$$

and

$$\left\langle \hat{X}_1^2 \right\rangle = \frac{1}{4} + \left\langle \hat{X}_1 \right\rangle^2, \tag{2.37}$$

$$\left\langle \hat{X}_2^2 \right\rangle = \frac{1}{4} + \left\langle \hat{X}_2 \right\rangle^2. \tag{2.38}$$

Therefore, for a coherent state one have

$$\left\langle \left(\Delta\hat{X}_1\right)^2 \right\rangle \left\langle \left(\Delta\hat{X}_2\right)^2 \right\rangle = \frac{1}{16}. \tag{2.39}$$

2.2.3 Squeezed States

From the previous section, we know that the coherent state is a minimum uncertainty state, where the fluctuations of $\hat{X}_1$ and $\hat{X}_2$ quadratures are the same. However, there exist other minimum uncertainty states, and their quadratures are not the same. One can call one of these states the squeezed state $|\alpha, \xi\rangle$. For now I will focus on single-mode squeezed states. The squeezed states can be generated from a physical process called squeezing, where the squeeze operator is defined as

$$\hat{S}(\xi) = \exp\left[-\frac{1}{2}\xi\hat{a}^{\dagger 2} + \frac{1}{2}\xi^*\hat{a}^2\right], \tag{2.40}$$

where $\xi = re^{2i\phi}$ is the squeezing parameter. The squeezed state can be generated in two ways: either first squeeze then displace, or first displace then squeeze. More specifically,

$$|\alpha, \xi\rangle = \hat{S}(\xi)\hat{D}(\alpha)\,|0\rangle = \hat{D}(\alpha)\hat{S}(\xi)\,|0\rangle\,. \tag{2.41}$$

It is easy to show that the average photon number in $|\alpha, \xi\rangle$ is given by

$$\langle\alpha, \xi|\,\hat{N}\,|\alpha, \xi\rangle = \sinh^2 r + |\alpha|^2. \tag{2.42}$$

Here one can define $\hat{Y}_1 + i\hat{Y}_2 = (\hat{X}_1 + i\hat{X}_2)e^{-i\phi} = \hat{a}e^{-i\phi}$, so that the quantum fluctuations of $\hat{Y}_1$ and $\hat{Y}_2$ are given by

$$\left\langle \left(\Delta\hat{Y}_1\right)^2 \right\rangle = \frac{1}{4}e^{-2r}, \tag{2.43}$$

$$\left\langle \left(\Delta\hat{Y}_2\right)^2 \right\rangle = \frac{1}{4}e^{2r}. \tag{2.44}$$

By comparing Eq. (2.43) with Eq. (2.44) for the coherent state, one can see that one of the quadratures is squeezed, while the other one is anti-squeezed. Note that, when $\alpha = 0$, this special squeezed state is called squeezed vacuum state, which could also be expanded in the Fock state basis as

$$|0, \xi\rangle = \frac{1}{\sqrt{\cosh r}} \sum_{n=0}^{\infty} \frac{\sqrt{(2n)!}}{n!} \left(-\frac{1}{2}e^{i\phi}\tanh r\right)^n |2n\rangle\,. \tag{2.45}$$

Last but not least, the two-mode squeezing operator is given by

$$\hat{S}_2(\xi) = \exp(\xi^*\hat{a}\hat{b} - \xi\hat{a}^\dagger\hat{b}^\dagger), \tag{2.46}$$

where $\xi = |\xi|e^{i\theta}$. The simplest non-classical two-mode Gaussian state, which is called two-mode squeezed vacuum state, can be generated from the vacuum by a two-mode squeezing

operation, so that

$$|\xi\rangle_2 = \hat{S}_2(\xi)|0,0\rangle, \tag{2.47}$$

whereas in the Fock basis it can be expressed as

$$|\xi\rangle_2 = \frac{1}{\cosh\xi}\sum_{n=0}^{\infty}(-1)^n e^{i\theta}\tanh^n\xi|n,n\rangle. \tag{2.48}$$

The two-mode squeezed vacuum state is not a product of squeezed states in modes a and b, but rather it is correlated between them being a superposition of terms with the same number of photons in both modes.

2.2.4 Thermal State

Finally, another common light state that one will encounter is the thermal state. The density matrix of the thermal state is given by

$$\hat{\rho}_{\text{th}} = \frac{\exp(-\hat{H}\Big/k_BT)}{\text{Tr}\left[\exp(-\hat{H}\Big/k_BT)\right]}, \tag{2.49}$$

where $\hat{H} = \hbar\omega(\hat{a}^\dagger\hat{a} + \frac{1}{2})$. After some algebra, one can rewrite the density matrix of the thermal state as

$$\hat{\rho}_{\text{th}} = \sum_{n=0}^{\infty} P_n \left|n\right\rangle\left\langle n\right|, \tag{2.50}$$

where

$$P_n = \langle n|\,\hat{\rho}_{\text{th}}\,|n\rangle = \frac{1}{Z}\exp(-E_n/k_BT), \tag{2.51}$$

and

$$Z = \frac{\exp(-\hbar\omega/2k_BT)}{1-\exp(-\hbar\omega/k_BT)}. \tag{2.52}$$

Using

$$\exp(-\hbar\omega/k_BT) = \frac{\bar{n}}{1+\bar{n}}, \tag{2.53}$$

one can simplify the density matrix of the thermal state to

$$\hat{\rho}_{\text{th}} = \frac{\bar{n}}{1+\bar{n}} \sum_{n=0}^{\infty} \left(\frac{\bar{n}}{1+\bar{n}} \right)^n |n\rangle \langle n| . \tag{2.54}$$

Furthermore, one can calculate the fluctuation of the photon number of the thermal state as

$$\left\langle (\Delta \hat{n})^2 \right\rangle = \left\langle \hat{n}^2 \right\rangle - \langle \hat{n} \rangle^2 = \bar{n} + \bar{n}^2. \tag{2.55}$$

2.2.5 Wigner Function of States

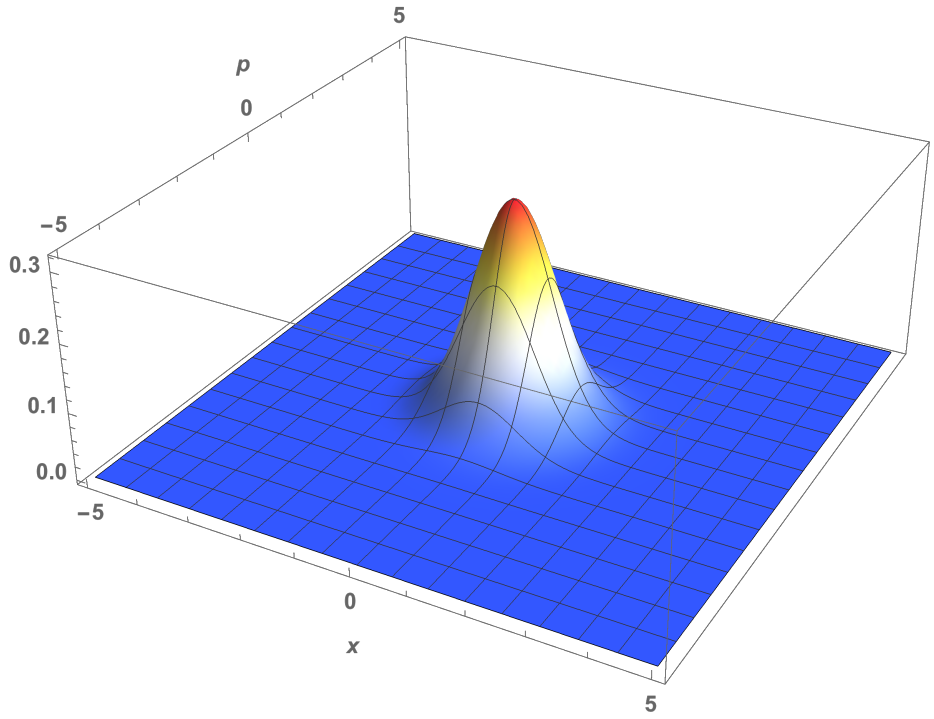

Figure 2.1: Wigner function of the vacuum state. It is a Gaussian-shaped distribution centered at the origin of the phase space.

Since $\hat{a}^\dagger$ and $\hat{a}$ can be written in terms of the phase-space operators $\hat{x}$ and $\hat{p}$, it is easy to show that different states can also be represented in phase-space. More specifically, one can use the Wigner function to describe different quantum states. The Wigner distribution is a quasi-probability distribution, since values of the Wigner function can be negative, which is not possible in classical probability theory. The definition of the Wigner function

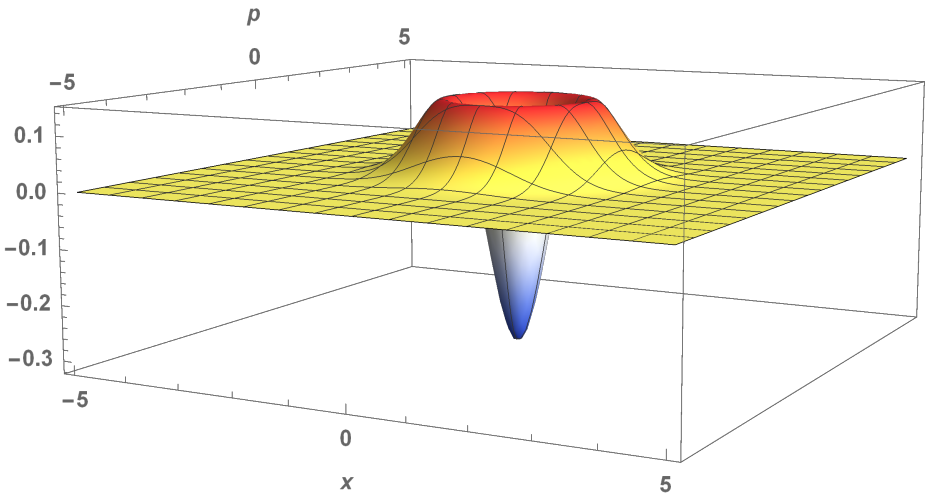

Figure 2.2: Wigner function of single photon Fock state. One can see that near the center of the phase space, the value of the Wigner function becomes negative, which indicates the quantumness of the Fock state.

is given by

$$W(x,p) = \frac{1}{2\pi}\int_{-\infty}^{\infty} \left\langle x + \frac{\nu}{2}\middle|\rho\middle| x - \frac{\nu}{2}\right\rangle e^{-ip\nu} d\nu = \mathrm{Tr}[\rho\Delta(x,p)], \tag{2.56}$$

where

$$\Delta(x,p) = \int_{-\infty}^{\infty} \frac{d\nu}{2\pi} e^{ip\nu} \left|x + \frac{\nu}{2}\right\rangle \left\langle x - \frac{\nu}{2}\right| \tag{2.57}$$

is the Wigner operator. From the equation above, one can see that the Wigner function is a function that describes the quantum distribution in classical phase space. If one integrates the momentum p, then the probability of getting the position x is given by

$$P(x) = \frac{1}{2\pi}\int_{-\infty}^{\infty} W(x,p)dp. \tag{2.58}$$

Accordingly, one can calculate the probability of getting momentum p as

$$P(p) = \frac{1}{2\pi}\int_{-\infty}^{\infty} W(x,p)dx. \tag{2.59}$$

To begin with, I will provide the Wigner function for some of the quantum states I

discussed above. For the vacuum state

$$W_{|0\rangle}(x,p) = \frac{1}{\pi} e^{-x^2-p^2}. \tag{2.60}$$

For the Fock state

$$W_{|n\rangle}(x,p) = \frac{1}{\pi}(-1)^n L_n[2(x^2+p^2)] e^{-x^2-p^2}, \tag{2.61}$$

where L_n are Laguerre polynomials, which satisfy

$$\sum_{n=0}^{\infty} L_n(x) z^n = (1-z)^{-1} \exp\left(\frac{xz}{z-1}\right). \tag{2.62}$$

Also note that, when $n = 0$, one gets back the Wigner function of the vacuum state. In Fig. 2.2, one can see that the Wigner function of the Fock state goes negative, which also represents the quantumness of the Fock state. For the coherent state,

$$W_{|\alpha\rangle}(x,p) = \frac{1}{\pi} e^{-\left(x-\sqrt{2}|\alpha|\cos\theta\right)^2 - \left(p-\sqrt{2}|\alpha|\sin\theta\right)^2}. \tag{2.63}$$

In Fig. 2.3, one can see that the Wigner function of the coherent state is the displaced vacuum.

For the single-mode squeezed vacuum state, when the squeezing phase is $\theta = \pi$, one have

$$W_{|0,\xi\rangle}(x,p) = \frac{1}{\pi} e^{-\frac{1}{2}x^2 e^{-2r} - \frac{1}{2}y^2 e^{2r}}. \tag{2.64}$$

As shown in Fig. 2.4, the Wigner function of the single-mode squeezed vacuum state no longer has a circularly symmetric shape. Rather, it is squeezed along a direction specified by the squeezing angle.

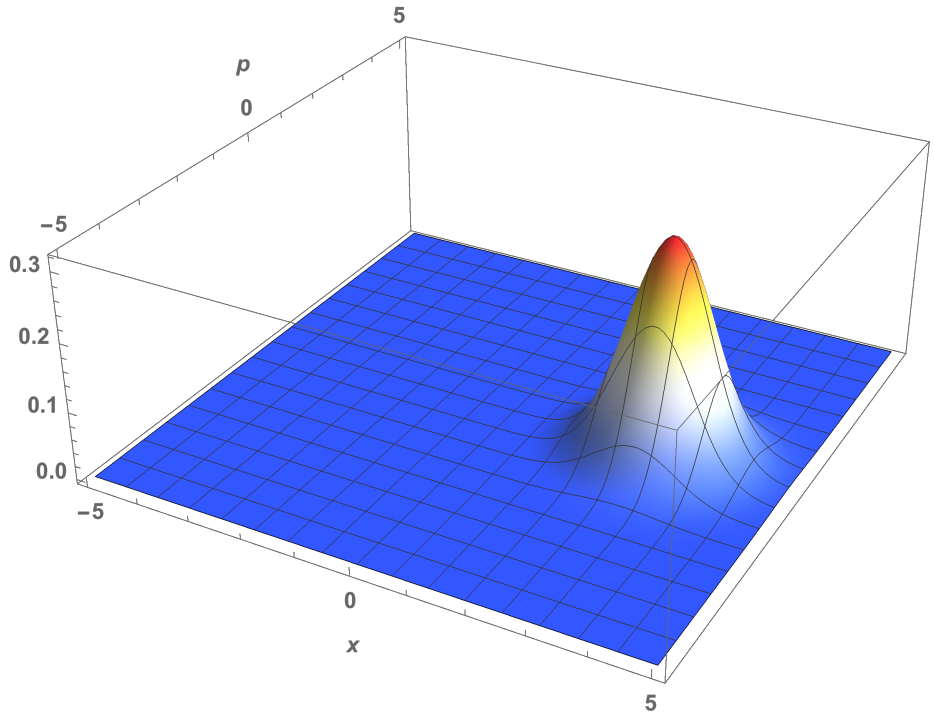

Figure 2.3: Wigner function of the coherent state. Here, $\alpha = 2$. Thus, the Wigner function of the coherent state is just the Wigner function of the vacuum state shifted along the x-axis by $\sqrt{2}\alpha \approx 2.82$ units.

And finally, for the thermal state

$$W_{|\text{th}\rangle}(x,p) = \frac{1}{\pi\left(\bar{n}+1\right)} e^{\frac{-x^2-p^2}{\bar{n}+1}}. \tag{2.65}$$

2.3 Quantum Metrology

2.3.1 Basic Example of Metrology

Here, let me start the discussion of quantum metrology by discussing the most basic model of the Mach-Zehnder interferometer, which is shown in Fig. 2.6. Two input states ρ_1 and ρ_2 interfere on the first beam-splitter (BS), then interact with two unknown phases θ and δ, then again interfere on another BS, and finally reach the detector 1 and detector 2. The metrology task is to estimate the phase difference between the two arms, namely, $\phi = \theta - \delta$.

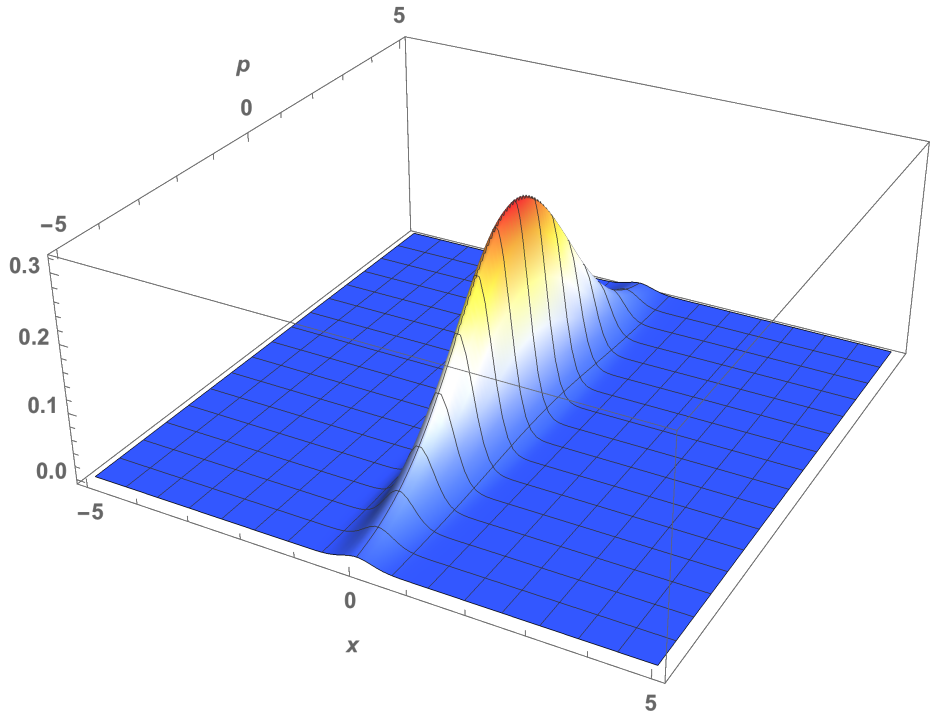

Figure 2.4: Wigner function of the single-mode squeezed vacuum state. Here, $r = 1$ and, since the squeezing angle is already fixed to π, the squeezing is along the p axis.

The action of the MZI can be analyzed with the Jordan-Schwinger representation in terms of the algebra of the angular momentum operators. Let us define the operators

$$\hat{J}_x = \frac{1}{2}(\hat{a}^\dagger \hat{b} + \hat{b}^\dagger \hat{a}), \hat{J}_y = \frac{1}{2}(\hat{b}^\dagger \hat{a} - \hat{a}^\dagger \hat{b}), \hat{J}_z = \frac{1}{2}(\hat{a}^\dagger \hat{a} - \hat{b}^\dagger \hat{b}). \tag{2.66}$$

In this definition, a balanced beam splitter is a rotation around the x axis by $\pi/2$: $U = \exp[-i\frac{\pi}{2}\hat{J}_x]$, and the phase delay is a φ rotation around the z axis, with $U = \exp[-i\varphi\hat{J}_z]$. For the most standard metrology task, one can use a measurement of the photon-number difference at the output, which is equivalent to $\hat{J}_z$ measurement as $\hat{n}_A - \hat{n}_B = 2\hat{J}_z$.

Then the precision of estimating φ can now be quantified via a simple error-propagation formula:

$$\Delta\varphi = \frac{(\Delta J_z)}{\left|\frac{d\langle \hat{J}_z \rangle}{d\varphi}\right|}. \tag{2.67}$$

With the input state as $|\alpha\rangle|0\rangle$ in mode A and mode B in Fig. 2.6, by using the error

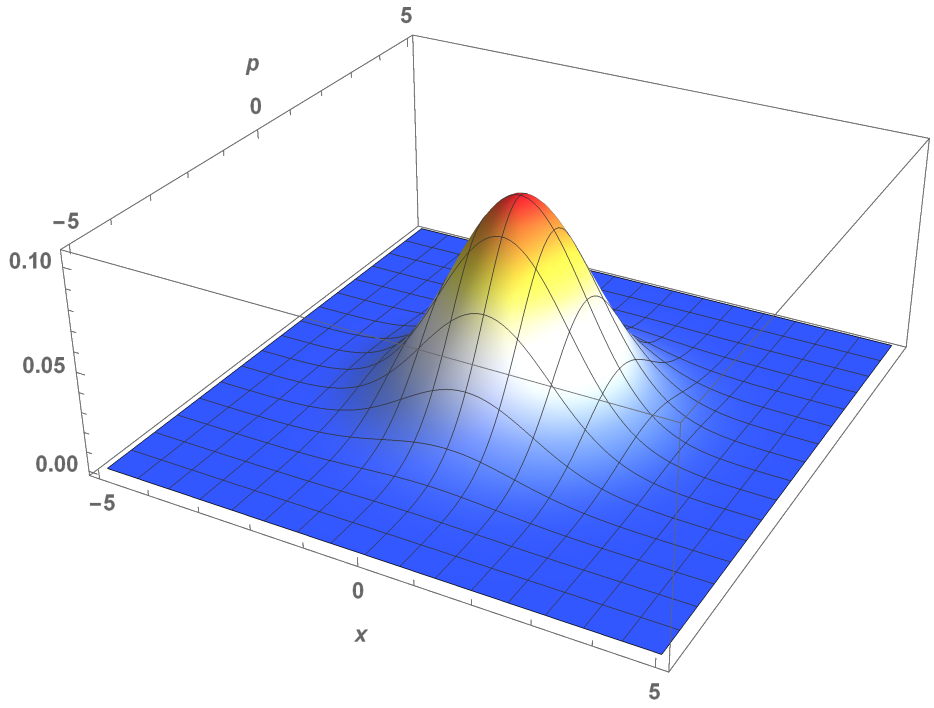

Figure 2.5: Wigner function of the thermal state. One can see that the shape is also Gaussian but it is larger than the vacuum state.

propagation method with intensity different measurement, where $\hat{O} = \hat{a}^\dagger\hat{a} - \hat{b}^\dagger\hat{b}$, one has $(\Delta O) = |\alpha|$ and $\left|\frac{d\langle\hat{O}\rangle}{d\varphi}\right| = |\alpha|^2 \sin\varphi$. Then the precision becomes

$$\Delta\varphi = \frac{1}{|\alpha \sin\varphi|} = \frac{1}{\sqrt{\langle N\rangle}|\sin\varphi|}, \tag{2.68}$$

where the average photon number is $\bar{N} = |\alpha|^2$. When $\varphi = \pi/2$, one obtains the so-called shotnoise limit (SNL).

Even though the error propagation formula is very easy to understand, the calculated precision depends on the actual measurement scheme. That is to say, if one needs to find the best precision of an interferometer, one needs to determine an optimal measurement, which is nearly impossible to do, since there could be infinite number of different measurement schemes.

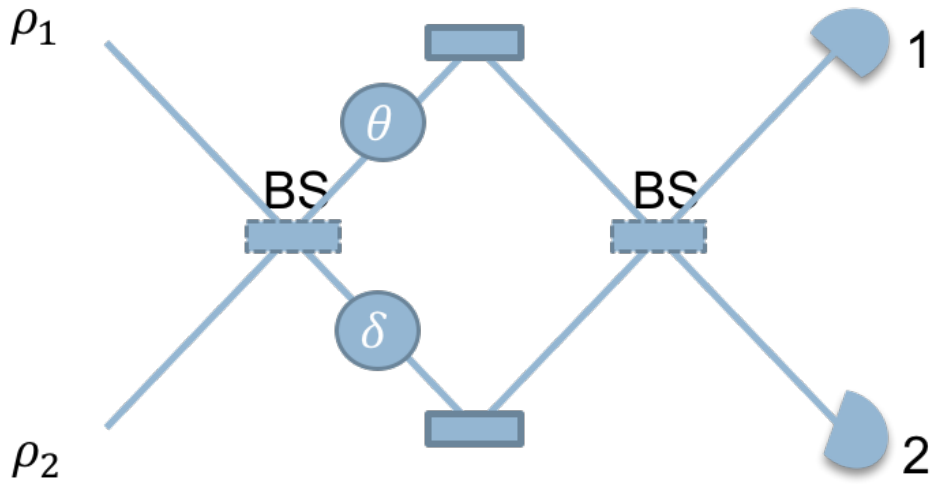

Figure 2.6: The Mach-Zehnder interferometer with two input light modes a, b, and two output modes a', b'. In a standard configuration, a coherent state of light $|\alpha\rangle$ is sent into mode a. In order to obtain quantum enhancement, one needs to make use of the b input port also, sending e.g. the squeezed vacuum state $|\xi\rangle$.

2.3.2 Classical Estimation Theory

Classically, one has a data set which consists of N copies of independent identically distributed random variables drawn from a probability density function (PDF), $p_\varphi(X)$, where the PDF is solely depending on an unknown parameter ϕ to estimate. Then the goal of the estimation is to construct an estimator $\tilde{\varphi}_N(\mathbf{x})$ to get the most accurate estimation. One approach is to use the Fisher information to determine such an optimal estimator.

One could construct the classical *Cramér-Rao Bound* (CRB) that lower-bounds the MSE of any unbiased estimator $\tilde{\varphi}_N$:

$$\Delta^2\tilde{\varphi}_N \geq \frac{1}{N\,F[p_\varphi]}\,, \tag{2.69}$$

where F is the *Fisher Information* (FI), which can be calculated as follows:

$$F\left[p_\varphi\right] = \int \mathrm{d}x\, \frac{1}{p_\varphi(x)} \left[\frac{\partial\, p_\varphi(x)}{\partial\varphi}\right]^2. \tag{2.70}$$

2.3.3 Quantum Estimation Theory

The *Quantum Cramér-Rao Bound* (QCRB) is the quantum generalization of the classical CRB, which sets the lower bound of the variance of estimation for all possible locally unbiased estimators and the most general measurements:

$$\Delta^2\varphi_N \geq \frac{1}{N\,F_{\mathrm{Q}}[\rho_\varphi]} \qquad \text{with} \qquad F_{\mathrm{Q}}[\rho_\varphi] = \mathrm{Tr}\big\{\rho_\varphi\, L[\rho_\varphi]^2\big\}\,. \tag{2.71}$$

For pure states $\rho_\varphi = |\psi_\varphi\rangle\langle\psi_\varphi|$, the QFI simplifies to

$$F_Q = 4(\langle\dot{\psi}_\varphi|\dot{\psi}_\varphi\rangle - |\langle\dot{\psi}_\varphi|\psi_\varphi\rangle|^2), \quad |\dot{\psi}_\varphi\rangle = \frac{d|\psi_\varphi\rangle}{d\varphi}. \tag{2.72}$$

Even better, in common cases, specifically in the context of optical interferometry, when the estimated parameter is encoded on the state by a unitary,

$$\rho_\varphi = U_\varphi \rho U_\varphi^\dagger, \quad U_\varphi = \mathrm{e}^{-\mathrm{i}\hat{H}\varphi}, \tag{2.73}$$

for the pure state estimation case, $\rho = |\psi\rangle\langle\psi|$, the QFI is proportional to the variance of $\hat{H}$:

$$F_Q(|\psi_\varphi\rangle) = 4\Delta^2 H = 4(\langle\psi|\hat{H}^2|\psi\rangle - \langle\psi|\hat{H}|\psi\rangle). \tag{2.74}$$

However, it is important to point out that sometimes QFI calculation results can be misleading. Since QFI optimizes over all possible measurement schemes, it could potentially include some cases that one has prior knowledge of the parameter one is trying to estimate beforehand. Thus, in order to make sure the QFI calculation is valid and possible, one needs to specify a measurement which could attain the QCRB set by QFI.

By utilizing the QFI method, one can then examine if a quantum state could help us. With the input state as $|\alpha\rangle|\xi\rangle$ in mode A and mode B in Fig. 2.6, one can then calculate

the QFI of the setup, which is given by

$$\Delta^2\phi = \frac{1}{|\alpha|^2 \mathrm{e}^{2r} + \sinh^2 r}. \tag{2.75}$$

The SNL for this setup is given by

$$\Delta^2\phi_{\mathrm{SNL}} = \frac{1}{N_{\mathrm{tot}}} = \frac{1}{|\alpha|^2 + \sinh^2 r}. \tag{2.76}$$

One can see that for any $r > 0$, $\Delta^2\phi < \Delta^2\phi_{\mathrm{SNL}}$. Thus, one can say that by using a quantum state, one can beat the SNL and achieve better sensitivity. Furthermore, when the squeezing $\xi = 0$, one gets back the result that I mentioned at the beginning of this section:

$$\Delta^2\phi = \frac{1}{|\alpha|^2}, \tag{2.77}$$

Therefore, by using QFI, one can easily find the best precision of an interferometer without determining a measurement.

2.4 Summary

In this chapter, the quantization of the electromagnetic field is reviewed, and then different states of light are presented and discussed. Furthermore, the basics of classical estimation theory and quantum estimation theory are discussed. These definitions and tools will be useful in the next chapters, where I discuss the conclusive precision limit of two-mode interferometers and multimode interferometers.

Chapter 3
Conclusive Precision Bounds of Two-Mode Interferometers

3.1 Introduction

Metrology, like other fields in physics, has been re-investigated by laws of quantum mechanics. The fundamental setup of a metrology device is a Mach-Zehnder interferometer (MZI). MZIs are widely used in the study of phase estimation. By utilizing only classical resources, the precision of estimation or sensitivity of this device is bounded by $\Delta^2\phi \geq 1/\bar{n}$, where $\bar{n}$ is the average photon number inside the interferometer. This bound is referred to as the shotnoise limit (SNL) [8]. However, this is not the ultimate limit. If one deploys quantum resources, then one can beat the SNL and reach the Heisenberg limit (HL), $\Delta^2\phi \geq 1/\bar{n}^2$ [8]. The estimation precision of the interferometer can be given by the error propagation formula for a given measurement scheme [13]. However, this approach cannot determine the optimal sensitivity without optimizing over all possible measurement schemes. To circumvent this problem, Braunstein and Caves introduced quantum Fisher information (QFI), which depends only on the input state and not on a particular measurement scheme [14]. The ultimate precision bounds of the phase sensitivity is then given by the quantum Cramér-Rao (QCRB) bound [14, 15], $\Delta^2\phi \geq 1/F_Q$, where F_Q is the QFI. For MZI, where all elements in the setup are passive, the SNL can be beaten by use of exotic quantum states: squeezed states [8], N00N states [9], twin Fock states [10] and two-mode squeezed states [11] [1].

Particularly, in Ref. [8], if the MZI is fed with a strong coherent state of light in one input port and vacuum in the other, then such a design would always only ever achieve the shotnoise limit (SNL). Then it is showed if you put squeezed vacuum into the unused port, you could beat the SNL. Several implementations of this squeezed vacuum scheme have

[1] This chapter is partially based on the contents of: Takeoka, M., Seshadreesan, K. P., You, C., Izumi, S., & Dowling, J. P. "Fundamental precision limit of a Mach-Zehnder interferometric sensor when one of the inputs is the vacuum." Phys. Rev. A 96.5 (2017): 052118. Reprinted by permission the American Physics Society. http://journals.aps.org/copyrightFAQ.html

already been demonstrated in the GEO 600 gravitational detector, and plans are underway to utilize this approach in the LIGO and VIRGO detectors in the future [16, 17].

It then appeared, that in the lore of quantum metrology, this result was extended — without proof — to the following no-go theorem: *If you put quantum vacuum into one input port of a balanced MZI, then no matter what quantum state of light you put into the other input port, and no matter what your detection scheme, the sensitivity can never be better than the SNL.* Often the proof of this theorem is cited to be the original 1981 paper by Caves [8], but upon further inspection, no such general claim is made there. A quantum-Fisher-information-based proof of this no-go theorem appeared in Pezzé and Smerzi [18], Lang and Caves [19], and later in Liu et al., [20], but is not explored in full generality as I do here.

The statement proved here is the following: *If the unknown-phase-shifts are in both the arms of the MZI, then the no-go theorem holds no matter whether the MZI is balanced or not. However, if the unknown phase shift is in only one of the two arms, then the no-go theorem does not hold.* The two models for the unknown phase shift unitary operation in the MZI are known to yield different values for the QFI in estimating the phase difference between the two arms [21, 22]. This discrepancy has been thought of as a flaw in the interpretation of the QFI [21], or being related to assumptions made about the input states and the measurements [22]. In contrast, here I point out that the two phase shift unitaries correspond to physically different types of sensors, and that their choice should depend on the concrete application scenario. The model where the unknown phase shift is in both the arms corresponds intrinsically to a two-parameter estimation problem. In this case, I prove that the no-go theorem holds, independently of whether the MZI is balanced or not, by carefully considering the phase-sum parameter (often regarded as the "global phase") along with the phase difference.

The other way of beating SNL is to use active elements in an interferometer. One of such interferometer is called a SU(1,1) interferometer, introduced by Yurke in 1986 [12],

where the beam splitters in the MZI are replaced by an active element, such as an optical parametric amplifier (OPA) or a four-wave mixers, which are mathematically characterized by the group SU(1,1). These interferometers can achieve Heisenberg sensitivity even if inputs are both vacua. Since first proposed, the phase sensitivity of the SU(1,1) interferometer has been extensively studied both in theory and experiment. Plick *et al.* [23] showed that coherent state inputs with intensity measurement could achieve higher sensitivity which was experimentally demonstrated by Ou [24]. Li *et al.* [25, 26] calculated the phase sensitivity of the SU(1,1) interferometer with coherent and squeezed vacuum states as inputs and homodyne and parity measurement as detection when the unknown phase shift is applied in one of the arms. They gave the QFI-based analysis as well. Gong *et al.* [27] also did the QFI analysis for coherent and squeezed states where the unknown phase shifts are applied in both arms. More recently, there has been an interest in other variant termed as pumped-up and truncated SU(1,1) [28, 29, 30, 31].

One issue in the SU(1,1) interferometer is that the QFI gives different precision limits with different configurations of the unknown phases, even for the same physical setup. For example, as mentioned recently by Gong et al. [27], three different phase configurations would yield three different QFIs with the same setup for most of the Gaussian state inputs. This issue was also observed in the MZI setting, and Jarzyna and Demkowicz-Dobrzański [21] pointed out that without proper consideration of external phase reference, the physically same setup lead to different QFIs in MZI. That is, naive calculation of QFI sometimes misleadingly overestimates the precision limit in the sense that, to achieve it, one requires *hidden* uncounted resource in measurement. They also proposed a technique to rule out these hidden resources by averaging the phase of the input states. Related to this, a rigorous justification of the fundamental precision limit of the MZI when one of the inputs is a vacuum was recently discussed [32].

The chapter is organized as follows. In Sec. 3.2, I will introduce the model and revisit the QFI analysis of the MZI and SU(1,1) interferometer with various input states and

unknown-phase models and point out the inconsistencies in the precision limits. In Sec. 3.3, to rule out the use of extra resources (phase and power), I use the phase averaging method to calculate the QFI when inputs are arbitrary state and a vacuum state. Our result unifies the inconsistencies in the QFIs and gives tighter result than previous analysis. In Sec. 3.4 I first draw connections between phase averaging method and multi-parameter estimation approach. I show that these two methods give identical results for this particular inputs. Furthermore, the bound I derive is valid even allowing external resources. In Sec. 3.5, using multi-parameter estimation approach, I derived precision bounds for two non-vacuum inputs in SU(1,1) interferometer and give tighter bounds than previously reported. Finally, in Sec. 3.6 I will summarize our results.

3.2 Model and Previous Work

3.2.1 MZI Model

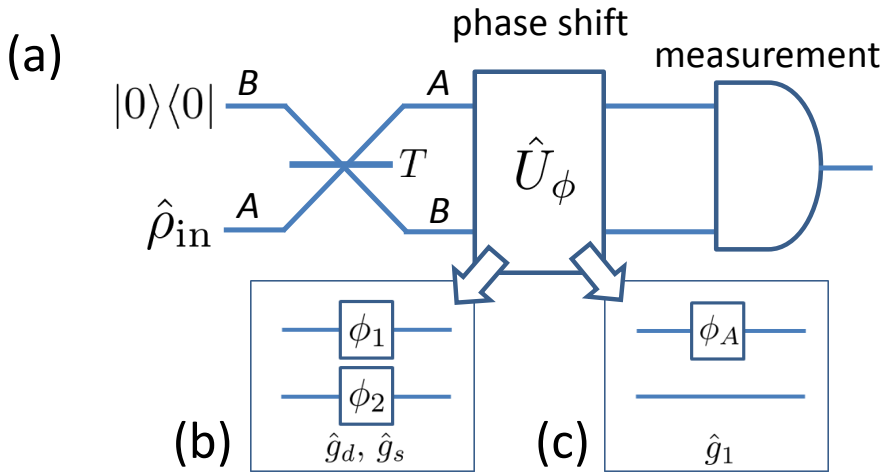

Figure 3.1: (a) Mach-Zehnder interferometer phase estimation, and the two different phase shift models: phase shift(s) are applied in (b) two arms, or (c) one arm of the interferometer.

A schematic of the Mach-Zehnder (MZ) interferometer based sensing setup I consider is illustrated in Fig. 3.1 (a). Two input modes A and B are interfered via a beam splitter with transmittance T, and then put into the phase shift unitary operation $\hat{U}_\phi$ followed by some measurement. In addition to this standard setting, I restrict one of the input states to always be the quantum vacuum state, whereas the other input can be an arbitrary quantum

state (possibly mixed).

A similar setup was considered by Lang and Caves [19] (see also Refs [18, 20]), with inputs in a tensor product of an arbitrary pure state $|\chi\rangle$ and a coherent state $|\alpha\rangle$, and a beam splitter of transmittance $T = 1/2$. They considered the phase shift unitary operator $\hat{U}_\phi = e^{i\hat{g}_s\phi_s}e^{i\hat{g}_d\phi_d}$ as shown in Fig. 3.1 (b), where ϕ_s and ϕ_d are the phase sum and difference of the two modes, respectively, $\hat{g}_s = (\hat{a}^\dagger\hat{a} + \hat{b}^\dagger\hat{b})/2$, $\hat{g}_d = (\hat{a}^\dagger\hat{a} - \hat{b}^\dagger\hat{b})/2$. These two phase shift parameters reflect the unknown phase shifts in the two arms of the MZI, ϕ_1 and ϕ_2, as $\phi_s = \phi_1 + \phi_2$, $\phi_d = \phi_1 - \phi_2$ (see Fig. 3.1(b)). $\hat{a}^\dagger$ ($\hat{b}^\dagger$) and $\hat{a}$ ($\hat{b}$) are creation and annihilation operators in mode A (B), respectively.

Then the authors showed that for a coherent state input with $\alpha = 0$, i.e. for the vacuum input, the quantum Fisher information (QFI) for the phase difference turns out to be the average photon number of the input:

$$F_Q(|\chi\rangle, \hat{g}_d) = \langle\chi|\hat{n}|\chi\rangle = \bar{n}_\chi, \tag{3.1}$$

where $\hat{n} = \hat{a}^\dagger\hat{a}$. This result suggests that the precision of the phase sensing is shotnoise limited when one of the input ports contains only vacuum (and the other mode contains any pure state), since the QCRB is $\Delta^2\phi \geq 1/F_Q$.

The above result still leaves open questions such as, does the no-go theorem hold when the interferometer is not balanced? and does it also hold when the phase shift unitary operator is chosen differently?

3.2.2 No-go theorem extended: Preliminary analysis

Firstly, for the phase shift unitary operator $\hat{g}_d$, when T deviates from 1/2, the QCRB already appears to beat the SNL. Keeping T as a free parameter, and using the fact that the QFI of a pure state in estimating a phase shift generated by a generator $\hat{g}$ is given by

$4\left(\langle\hat{g}^2\rangle - \langle\hat{g}\rangle^2\right)$, one arrives at

$$F_Q(|\chi\rangle, \hat{g}_d, T) = \{1-(1-2T)^2\}\bar{n}_\chi + (1-2T)^2 V_\chi. \tag{3.2}$$

(See Appendix B for the derivation.) This beats the SNL for any non-50/50 beam splitter quite spectacularly. For example, with $T \to 0$, the QCRB approaches $\Delta^2\phi = 1/V_x < 1/\bar{n}_\chi$ for some inputs such as squeezed vacuum [11].

Secondly, as pointed out and rigorously discussed in Ref. [21], a different choice of the phase shift unitary can give a different value for the QFI. For example, in lieu of the phase shift operator $\hat{g}_d$, one can instead choose $\hat{U}_\phi = e^{i\hat{g}_1\phi_A}$, where $\hat{g}_1 = \hat{a}^\dagger\hat{a}$, such that phase shift is generated only in one arm. The QFI for the phase shift unitary operator $\hat{g}_1$ is found to be

$$F_Q(|\chi\rangle, \hat{g}_1) = \bar{n}_\chi + V_\chi, \tag{3.3}$$

where $V_\chi = \langle\chi|\hat{n}^2|\chi\rangle - \langle\chi|\hat{n}|\chi\rangle^2$ is the photon number variance of $|\chi\rangle$ (see Appendix B for the derivation). This is obviously different from Eq. (3.1), and again implies a sub-SNL result, since $V_\chi > \bar{n}_\chi$ is possible for some inputs, as mentioned above.

These results, extrapolated from Ref. [19], are thus perplexing [2], since seemingly both Eqs. (3.2) and (3.3) suggest the possibility of sub-SNL precision phase sensing even with vacuum input into one of the input ports.

3.2.3 SU(1,1) Model

A schematic of the SU(1,1) interferometer is shown in Fig. 3.2. Two input modes interact via optical parametric amplifier (OPA) with gain parameter g, and then go through a phase shift on one or both of the arms. After the phase shifts, the measurement is performed. Note that the measurement often consists of a second OPA with pumping of π phase difference than the first one followed by detectors.

[2] Note that Refs. [18, 20] also suggest no-go arguments, but do not resolve these problems.

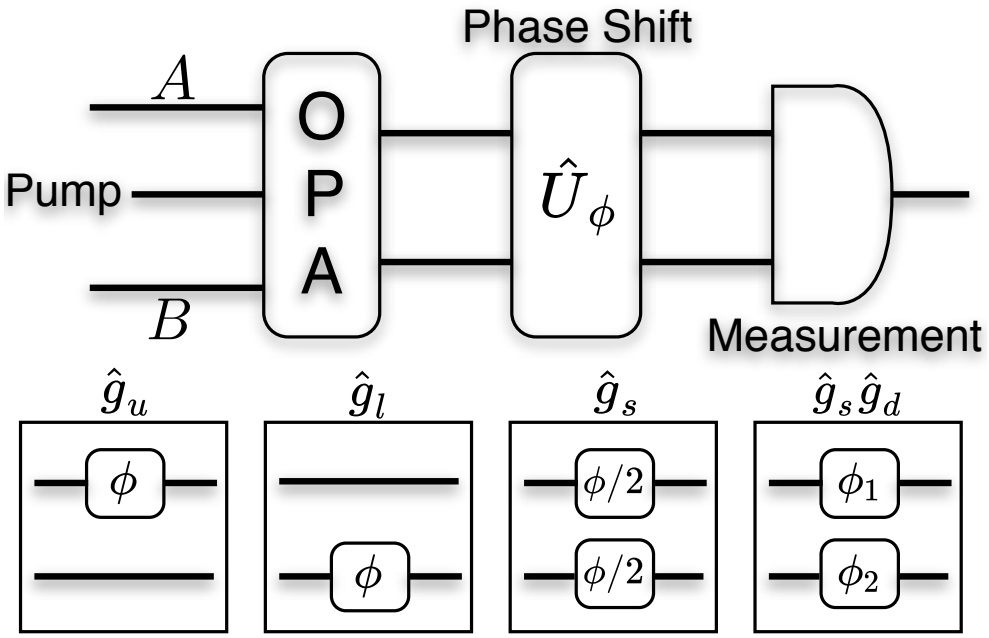

Figure 3.2: Schematic of a SU(1,1) interferometer with different phase shift models: phase shift in upper arm only ($\hat{g}_u$ model), phase shift in lower arm only ($\hat{g}_l$ model), phase shift equally splitted in both arms ($\hat{g}_s$ model), unknown phase shifts in both arms ($\hat{g}_s - \hat{g}_d$ model).

The relation between the output and input modes of the OPA is given by:

$$\begin{aligned} \hat{a}_1 &= \cosh(g)\,\hat{a}_0 + \mathrm{e}^{\mathrm{i}\theta}\sinh(g)\,\hat{b}_0^\dagger, \\ \hat{b}_1 &= \cosh(g)\,\hat{b}_0 + \mathrm{e}^{\mathrm{i}\theta}\sinh(g)\,\hat{a}_0^\dagger, \end{aligned} \tag{3.4}$$

where $\hat{a}_i$ ($\hat{b}_i$) and $\hat{a}_i^\dagger$ ($\hat{b}_i^\dagger$) are the annihilation and creation operators in mode A (B), respectively, and the subscripts 0 and 1 represent the input and the output of the OPA, respectively (see Fig. 3.2). g and θ are the parametric gain and phase of the OPA, respectively.

The unknown phase shifts to be estimated are modeled in different ways. The choice of the models depend on what type of application scenario one has in mind [32]. When the unknown phase shift ϕ occurs only in the upper arm, it is modeled by unitary operation $\hat{U}_\phi^u = \mathrm{e}^{\mathrm{i}\hat{g}_u\phi}$ with generator $\hat{g}_u = \hat{a}_1^\dagger\hat{a}_1$. If the phase shift is in only in the lower arm, one has $\hat{U}_\phi^l = \mathrm{e}^{\mathrm{i}\hat{g}_l\phi}$ with generator $\hat{g}_l = \hat{b}_1^\dagger\hat{b}_1$. Sometimes, the unknown phase shift is equally split into two arms, then $\hat{U}_\phi^s = \mathrm{e}^{\mathrm{i}\hat{g}_s\phi}$ where $\hat{g}_s = (\hat{a}_1^\dagger\hat{a}_1 + \hat{b}_1^\dagger\hat{b}_1)/2$. In some applications,

different unknown phase shifts occur in the each arms. The unitary operator is then given by $\hat{U}_\phi = \mathrm{e}^{\mathrm{i}\hat{g}_1\phi_1}\mathrm{e}^{\mathrm{i}\hat{g}_2\phi_2} = \mathrm{e}^{\mathrm{i}\hat{g}_s\phi_s}\mathrm{e}^{\mathrm{i}\hat{g}_d\phi_d}$, where $\hat{g}_d = (\hat{a}_1^\dagger\hat{a}_1 - \hat{b}_1^\dagger\hat{b}_1)/2$ and ϕ_1 and ϕ_2 are the unknown phases in the two arms. These phases are also described by the phase sum $\phi_s = \phi_1 + \phi_2$, and the phase difference $\phi_d = \phi_1 - \phi_2$. Note that the first three cases are basically a single-parameter estimation problem and the last one is a two-parameter estimation problem.

3.2.4 Review of the previous QFI approach

Here I review the previous QFI approach to determine the sensitivity bound for the single-parameter SU(1,1) interferometric sensing. When the state before the measurement is a pure state, $|\psi_\phi\rangle_{AB} = e^{-\mathrm{i}\hat{g}\phi}|\psi\rangle_{AB}$, the QFI is given by [14]

$$F_Q = 4(\langle\psi|\hat{g}^2|\psi\rangle - \langle\psi|\hat{g}|\psi\rangle^2). \tag{3.5}$$

By using Eq. (3.4) and Eq. (3.5), when the input states are both vacuum states, all different phase configurations yield the same QFI:

$$F_Q = n_\kappa(n_\kappa + 2), \tag{3.6}$$

where $n_\kappa = 2\sinh^2(g)$ is the average photon number of the output state. That is, the precision bound is independent of what model one chooses.

However, the situation starts to change when one of the input mode is not a vacuum state.

For example, in Ref. [27], the authors calculated the QFI from Eq. (3.5), where one input is a coherent state and the other is a coherent or squeezed state. To simplify, taking one input to be coherent state $|\beta\rangle$ with $n_\beta = |\beta|^2$ and the other to be a vacuum, the QFIs

in Ref. [27], for generators $\hat{g}_u$, $\hat{g}_l$, and $\hat{g}_s$ are reduced to,

$$F_Q(\hat{g}_u) = n_\beta \cosh 4g + \sinh^2 2g + n_\beta(1 - 2\cosh 2g), \tag{3.7}$$

$$F_Q(\hat{g}_l) = n_\beta \cosh 4g + \sinh^2 2g + n_\beta(1 + 2\cosh 2g), \tag{3.8}$$

$$F_Q(\hat{g}_s) = n_\beta \cosh 4g + \sinh^2 2g, \tag{3.9}$$

which suggests that a choice of the phase shift model changes the QCRB of the phase estimation even using the same physical setup. Then one may ask a question: do they reflect tight precision limits? In other words, is there any possibility of overestimating the bound by use of *hidden* resources at the measurement? In the next section, I show that after ruling out any external resources, the QCRBs are unified and tighter than any of the above bounds.

3.3 Single-phase Estimation with Vacuum and Arbitrary State

3.3.1 Mach-Zehnder Interferometer

The $\hat{g}_1$ model is a single-parameter estimation problem. Thus, (3.3) is directly applied to the QCRB, which suggests sub-SNL sensitivity with input states of high V_χ, i.e., states with high photon number fluctuation, e.g., squeezed vacuum. Then, as mentioned in the introduction, the QFI-only approach may have the pitfall that the optimal POVM attaining the QCRB might contain huge amount of hidden resources as pointed out by Jarzyna and Demkowicz-Dobrzański [21]. In other words, one might fool oneself into thinking, via the QFI-only approach, that there is some quantum metrological advantage, where none actually exists.

There are two remedies. The first is to rule out any external resource that might give some phase information to the measurement device in implementing the optimal POVM. Such a rule-out protocol was introduced by Jarzyna and Demkowicz-Dobrzański [21] where the issue is resolved by introducing the phase-averaging of the two-mode input state via a common phase shift. The QFI of the phase-averaged input gives the proper phase-sensing

limit without any external phase reference.

The second remedy, the one I recommend, is that if one wishes to claim a quantum metrological advantage from a QFI-only calculation, then a detection scheme that actually hits the related QCRB must be provided, so that all resources hidden in the associated POVM may be laid bare for all to see. This allows one to fairly count all the resources used in the interferometer. (For example, in Ref. [11], the QFI calculation is backed up by providing a detection scheme, the parity operator, hitting the QCRB).

Here I apply these two remedies separately. First, I employ the phase-averaging approach [21] to eliminate any hidden resource in the POVM. I briefly sketch the calculation in the following and describes the details in Appendix D. Consider the input state of $\hat{\rho}_{\rm in} \otimes |0\rangle\langle 0|$ where $\hat{\rho}_{\rm in} = \sum_{n,m}^{\infty} c_{nm}|n\rangle\langle m|$ is an arbitrary state and $|n\rangle$ is the n-photon number basis. The phase-averaging operation drops off its non-diagonal terms. After the phase-averaging, the first beamsplitter and the ϕ phase shifting, the input is transformed to $\Psi^{\phi}_{\rm avg} = \sum_{n=0}^{\infty} p_n |\psi_n(\phi)\rangle\langle\psi_n(\phi)|_{AB}$, where $|\psi_n(\phi)\rangle$ and $|\psi_{n'}(\phi)\rangle$ are orthogonal for $n \neq n'$.

By using the convexity of the QFI and the above orthogonality, I have $F_Q^{(1)}\left(\Psi^{\phi}_{\rm avg}\right) = \sum_{n=0}^{\infty} p_n F_Q^{(1)}\left(|\psi_n(\phi)\rangle\right)$, and after some calculations, one sees $F_Q^{(1)}\left(|\psi_n(\phi)\rangle\right) = 4nT\left(1-T\right)$, which is maximized at $T = 1/2$, and is equal to n, as it should be (see Appendix D). Consequently, the QFI for $\Psi^{\phi}_{\rm ave}$ is given as

$$F_Q\left(\Psi^{\phi}_{\rm avg}\right) = \sum_{n=0}^{\infty} n p_n = \bar{n}, \tag{3.10}$$

where $\bar{n}$ is the average photon number of $\hat{\rho}_{\rm in}$, and thus one finds that the phase sensitivity is lower bounded as $\Delta^2\phi_A \geq 1/\bar{n}$. That is, if the optimal POVM is not allowed to have external phase information, the estimation precision is limited by the shotnoise limit.

3.3.2 SU(1,1) Interferometer

In this section, I consider a slightly more general situation than that in the previous section. I consider the single-phase estimation of the SU(1,1) interferometer where one

input (mode A) is an arbitrary state $\hat{\rho}_\chi$ and the other (mode B) is a vacuum $|0\rangle\langle 0|$.

As pointed out in Refs. [21, 32], the QFI-only approach sometime falsely suggests a quantum advantage, as the optimal measurement saturating the bound may include uncounted resources, such as an external strong local oscillator. The possibility of this overestimation is circumvented by eliminating the common reference frame between the input states and the measurement. Let us expand $\hat{\rho}_\chi$ in the photon-number basis:

$$\hat{\rho}_\chi = \sum_{n,m=0}^{\infty} c_{nm}|n\rangle\langle m|, \tag{3.11}$$

where $|n\rangle$ is the n-photon number state. The reference frame between the inputs and the measurement are removed by phase-averaging the input state as [21],

$$\begin{aligned}
\Psi_{\text{avg}} &= \int \frac{d\varphi}{2\pi} \hat{V}_\varphi^A \hat{V}_\varphi^B \left(\hat{\rho}_\chi^A \otimes |0\rangle\langle 0|^B\right) \hat{V}_\varphi^{A\dagger} \hat{V}_\varphi^{B\dagger} \\
&= \sum_{n,m=0}^{\infty} \int \frac{d\varphi}{2\pi} e^{i\varphi(n-m)} c_{nm} |n\rangle\langle m|^A \otimes |0\rangle\langle 0|^B \\
&= \sum_{n=0}^{\infty} p_n |n\rangle\langle n|^A \otimes |0\rangle\langle 0|^B,
\end{aligned} \tag{3.12}$$

where $\hat{V}_\varphi^A = e^{i\varphi \hat{a}^\dagger \hat{a}}$, $\hat{V}_\varphi^B = e^{i\varphi \hat{b}^\dagger \hat{b}}$, and $p_n = c_{nn}$ is a real positive number satisfying $\sum_n p_n = 1$ [32, 33].

The state after the first OPA is given by

$$\begin{aligned}
\Psi_{\text{avg}}^{\text{OPA}} &= \hat{T}_{\text{OPA}}^{AB} \Psi_{\text{avg}} \hat{T}_{\text{OPA}}^{\dagger AB} \\
&= \sum_{n=0}^{\infty} p_n \left(\hat{T}_{\text{OPA}}^{AB} |n\rangle\langle n|^A \otimes |0\rangle\langle 0|^B \hat{T}_{\text{OPA}}^{\dagger AB}\right) \\
&= \sum_{n=0}^{\infty} p_n |\psi_n\rangle\langle\psi_n|_{AB},
\end{aligned} \tag{3.13}$$

where

$$|\psi_n\rangle_{AB} = \sum_{k=0}^{\infty} c_{n,k} |k+n\rangle_A \otimes |k\rangle_B, \tag{3.14}$$

which follows from the fact that the photon number difference between two arms is conserved [12]. Note that $c_{n,k}$ is a function of the OPA phase θ. This means that one only averages the input phases but not the OPA phase θ. That is, one is allowed to use the reference frame θ and corresponding extra resources at the measurement step as it is in the original proposal of the SU(1,1) interferometric sensing [12].

By using the convexity of the QFI [34, 35] and noticing that $|\psi_n\rangle$ and $|\psi_{n'}\rangle$ are distinguishable for $n \neq n'$ after the phase shift, one has

$$F_Q\left(\Psi_{\text{avg}}\right) = \sum_{n=0}^{\infty} p_n F_Q\left(|\psi_n\rangle\right). \tag{3.15}$$

I justify the statement more carefully: in the lhs of Eq. (3.15), Ψ_{avg} is used as an input. Denote the state after the phase shift as $\Psi_{\text{avg}}(\phi) = \sum_n p_n |\psi_n(\phi)\rangle\langle\psi_n(\phi)|$. Then in principle, each $|\psi_n(\phi)\rangle$ contained in $\Psi_{\text{avg}}(\phi)$ is perfectly and coherently distinguishable by applying projectors $P_m = \sum_{j=0}^{\infty} |m+j\rangle\langle m+j| \otimes |j\rangle\langle j|$ (in other words, applying quantum non-demolition measurement on that basis). That is, one can distinguish $|\psi_n(\phi)\rangle$ in a post-selective way and then conditionally choose the measurement for phase estimation. This situation is basically the same as what is in the right hand side of Eq. (3.15), where one choose $|\psi_n\rangle$ *a priori* as an input with weight p_n and then apply appropriate measurements to each of them. Therefore, the right hand side of Eq. (3.15) is always reachable with Ψ_{avg}. Combining this fact with the convexity of the QFI, one obtains the equality in Eq. (3.15).

For the phase shift in upper arm only model $\hat{g}_u$, the QFI of $|\psi_n\rangle$ is given by

$$F_Q^u\left(|\psi_n\rangle\right) = 4(\langle \hat{g}_u^2 \rangle - \langle \hat{g}_u \rangle^2), \tag{3.16}$$

where

$$\langle \hat{g}_u \rangle = n \cosh^2(g) + \sinh^2(g), \tag{3.17}$$

and

$$\begin{aligned} \left\langle \hat{g}_u^2 \right\rangle &= n^2 \cosh^4(g) + (n+1) \cosh^2(g) \sinh^2(g) \\ &\quad + 2n \cosh^2(g) \sinh^2(g) + \sinh^4(g). \end{aligned} \tag{3.18}$$

Thus,

$$F_Q^u \left(|\psi_n\rangle \right) = 4(n+1) \sinh^2(g) \cosh^2(g) = (n+1) n_\kappa (n_\kappa + 2). \tag{3.19}$$

Consequently, the QFI of the phase-averaged input state is given by

$$\begin{aligned} F_Q^u \left(\Psi_{\text{avg}} \right) &= \sum_{n=0}^{\infty} p_n (n+1) n_\kappa (n_\kappa + 2) \\ &= (\bar{n}_\chi + 1) n_\kappa (n_\kappa + 2), \end{aligned} \tag{3.20}$$

where $\bar{n}_\chi = \sum_n n p_n$ is the average photon number of $\hat{\rho}_\chi$.

Similarly, for the phase shift in lower arm only model $\hat{g}_l$, the phase-averaged input state yields,

$$F_Q^l \left(\Psi_{\text{avg}} \right) = (\bar{n}_\chi + 1) n_\kappa (n_\kappa + 2). \tag{3.21}$$

Finally, for the equally-split phase shift model $\hat{g}_s$ one gets,

$$F_Q^s \left(\Psi_{\text{avg}} \right) = (\bar{n}_\chi + 1) n_\kappa (n_\kappa + 2). \tag{3.22}$$

The results in Eqs. (3.20–3.22) show that, once one rules out the use of external references (resources such as phase and power) at the measurement, all these models give the same QFI. Note that by taking $\bar{n}_\chi \to 0$, i.e. setting the two inputs both vacuum, one recovers Eq. (3.6).

When the input state in mode A is a coherent state $|\alpha\rangle$, one has

$$F_Q^{\alpha} = (n_\alpha + 1)n_\kappa(n_\kappa + 2). \tag{3.23}$$

This is tighter than any QFIs without phase-averaging mentioned in the previous section [Eqs. (3.8–3.9)]. That is, to achieve the QFIs in Eqs. (3.8–3.9), external (but uncounted) resources at the measurement are required. Note that our bound in Eq. (3.23) is tight in the sense that it is saturated by the parity detection [26].

From Eq. (3.20) one can see that, when one of the input is a vacuum, the QFI is proportional to $\bar{n}_\chi$ but does not depend on the structure of $\hat{\rho}_\chi$. This means that if one fixes the OPA gain g, then the best strategy is to use a state with higher average photon number. In other words, no nonclassicality of the input state can boost the sensitivity, when the other input is a vacuum. This situation has some similarity with the MZI case [32], where if one of the inputs is vacuum, one cannot beat the shotnoise limit by any nonclassical input from the other port. Also, if one restricts the total amount of resources used in both the input state and the OPA, then the best strategy is to concentrate all the power resource into the OPA.

3.4 Two-phase Estimation with Vacuum and Arbitrary State

3.4.1 Mach-Zehnder Interferometer

The MZI sensing with the $\hat{g}_s$-$\hat{g}_d$ model in its full generality is a two-parameter estimation problem since there are two unknown parameters, ϕ_s and ϕ_d, in the system. Although only the phase difference ϕ_d is of interest, this two-parameter model allows us to explicitly include the fact that one does not know ϕ_s in prior. This generally limits the precision limit of sensing ϕ_d especially when ϕ_d and ϕ_s are correlated. Therefore, a two-by-two quantum Fisher information matrix (QFIM) is considered. The problem in Eq. (3.2) is in fact due to the ignorance of the phase sum ϕ_s [3]. In multi-parameter estimation, the QCRB

[3] In Ref. [19], the QFIM of the system considered was calculated. However, they reduce it to the single-parameter estimation (i.e. drop off the terms for ϕ_s) which looses the tightness of the bound. Note that

is given by $\Sigma \geq \mathcal{F}_Q^{-1}$, where Σ is the covariance matrix of the estimator including both ϕ_s and ϕ_d and $\mathcal{F}_Q$ is the two-by-two QFIM:

$$\mathcal{F}_Q = \begin{bmatrix} F_{dd} & F_{sd} \\ F_{ds} & F_{ss} \end{bmatrix}, \tag{3.24}$$

where s and d correspond to ϕ_s and ϕ_d. The first diagonal element of $\mathcal{F}_Q^{-1}$ corresponds to the estimation limit of ϕ_d, which is explicitly given by

$$\frac{F_{ss}}{F_{ss}F_{dd} - F_{sd}F_{ds}}. \tag{3.25}$$

For an arbitrary mixed quantum state, the QFIM is in general not easy to calculate. However, the optimal input state that maximizes $\mathcal{F}_Q$ is always given by a pure-state input. This is the consequence of the convexity of the QFIM: for $\hat{\rho}_\phi = p\hat{\sigma}_\phi + (1-p)\hat{\tau}_\phi$,

$$\mathcal{F}_Q(\hat{\rho}_\phi) \leq p\mathcal{F}_Q(\hat{\sigma}_\phi) + (1-p)\mathcal{F}_Q(\hat{\tau}_\phi), \tag{3.26}$$

holds. This can be proved by using the monotonicity of the QFIM under the completely positive trace preserving (CPTP) map [36, 37] and extending the proof of the convexity for the QFI [38] (see Appendix C). The statement basically says that a statistical mixture of the input states will never increase the QFIM and thus implies that the QFIM is maximized with a pure state input. The optimal pure state for the QFIM is also optimal for the multi-parameter QCRB since the QFIM is a positive matrix and for positive matrices A and B, $B^{-1} \geq A^{-1}$ holds if and only if $A \geq B$.

Therefore, by considering a pure input state $|\chi\rangle$, the elements of the QFIM are given by

$$F_{ij} = 4\left(\langle \hat{g}_i \hat{g}_j \rangle - \langle \hat{g}_i \rangle \langle \hat{g}_j \rangle\right), \tag{3.27}$$

this problem does not appear in Eq. (3.1) since with $T = 1/2$, the non-diagonal term of the QFIM goes to zero and thus the problem reduces to two independent single-parameter estimations. Nevertheless, in Ref. [19], they also consider the non-vacuum input case where the bound may have some looseness.

where i, j takes s and d. We can calculate F_{dd}, F_{ss}, F_{ds}, and F_{sd} explicitly (see Appendix B. Note that F_{dd} corresponds to Eq. (3.2)) and then inserting these into (3.25), one gets

$$\Delta^2\phi_d \geq \frac{1}{4T(1-T)\bar{n}_\chi}, \tag{3.28}$$

where the minimum of the right hand side is obtained with $T = 1/2$ as $1/\bar{n}_\chi$, which is the SNL, as it should be. That is, no matter how highly nonclassical the input state $\hat{\rho}_{\text{in}}$ is, and no matter what POVM you deploy, the SNL cannot be surpassed for $\hat{g}_d$ so long as the other input to the interferometer is the vacuum state. Thus, this result establishes the no-go theorem in its most general form, which includes the beam splitter transmissivity as a free parameter.

3.4.2 SU(1,1) Interferometer

In the last section, I consider single-phase estimation and use the phase-averaging method to calculate the QFI of the SU(1,1) interferometer, where the input state is given by an arbitrary state and a vacuum state. For the $\hat{g}_u$ and $\hat{g}_l$ models, all the phase shift is located in only one of the arms. In other words, I assume that one knows there is no phase shift in the other arm.

The $\hat{g}_s$ only model is also a single-parameter estimation since one assumes the common unknown phase shift occurs in both arms. That is, one (implicitly) assumes that the phase difference $\phi_d = \phi/2 - \phi/2 = 0$ is known *a priori*. However, in many applications, different phase shift occurs in each arm, or equivalently, both the phase sum (ϕ_s) and phase difference (ϕ_d) are unknown. Then one needs to consider the two-parameter estimation problem, even if only one of them is of interest.

In this section, I consider the estimation of ϕ_s and ϕ_d with the SU(1,1) interferometer where again one input is an arbitrary state and the other is a vacuum. Without loss of generality, one can restrict the former to be a pure state $|\chi\rangle$ (this is justified by the convexity of the quantum Fisher information quantities, for example, see Ref. [32]).

The QCRB for multi-parameter estimation is calculated through the quantum Fisher information matrix (QFIM) [15, 39]. For the estimation of ϕ_d and ϕ_s, its QFIM is given by a two-by-two matrix:

$$\mathcal{F}_Q = \begin{bmatrix} F_{dd} & F_{sd} \\ F_{ds} & F_{ss} \end{bmatrix}, \tag{3.29}$$

where $F_{ij} = 4\left(\langle \hat{g}_i \hat{g}_j \rangle - \langle \hat{g}_i \rangle \langle \hat{g}_j \rangle\right)$ and the subscripts s and d denote ϕ_s and ϕ_d, respectively.

In the MZI case, one is usually interested in the estimation of only ϕ_d. Then its QCRB derived from the QFIM is given by [32, 21, 19, 40]

$$\Delta^2 \phi_d \geq \frac{F_{ss}}{F_{dd}F_{ss} - F_{ds}F_{sd}}. \tag{3.30}$$

Only when the beam splitter of the MZI is 50/50, do the off-diagonal elements vanish since $F_{sd} = F_{ds} = 0$, and then Eq. (3.30) simplifies to $\Delta^2 \phi_d \geq F_{dd}^{-1}$. That is, one does not need to care if ϕ_s is known a priori to find the ultimate precision limit of estimating ϕ_d. In general, however, one needs to take into account the full QFIM, i.e. the precision limit of estimating ϕ_d depends on the presence or absence of the information of ϕ_s.

The same situation is applied to the SU(1,1) interferometer.

Since the only interesting quantity to measure in the SU(1,1) interferometer is the phase sum ϕ_s, one is interested in the QCRB of ϕ_s:

$$\Delta^2 \phi_s \geq \frac{F_{dd}}{F_{dd}F_{ss} - F_{ds}F_{sd}}. \tag{3.31}$$

Applying our input states $|\chi\rangle \otimes |0\rangle$ into the QFIM elements for the SU(1,1) interferometer,

one has

$$F_{dd} = V_\chi, \tag{3.32}$$

$$F_{ds} = F_{sd} = V_\chi \cosh(2g), \tag{3.33}$$

$$F_{ss} = V_\chi \cosh^2(2g) + (1 + \bar{n}_\chi) \sinh^2(2g), \tag{3.34}$$

where $\bar{n}_\chi$ is the average photon number of state $|\chi\rangle$ and $V_\chi = \langle\chi|\hat{n}^2|\chi\rangle - \langle\chi|\hat{n}|\chi\rangle^2$ is the photon number variance of $|\chi\rangle$. Plugging them into Eq. (3.31), one gets

$$\Delta^2\phi_s \geq \frac{1}{(\bar{n}_\chi + 1)n_\kappa(n_\kappa + 2)}. \tag{3.35}$$

The above calculation reveals a critical role of the non-diagonal terms F_{ds} and F_{sd}. In fact, they contribute to cancel out V_χ from Eq. (3.35). As a consequence, the expression of Eq. (3.35) coincides with the one for the single-parameter estimation with the phase averaging [Eqs. (3.20–3.22)]. Thus any nonclassicality of $|\chi\rangle$ does not help to boost the sensitivity. Also it should be noted that if one ignore the non-diagonal terms, i.e. implicitly assuming that ϕ_d is known a priori, one could get higher QFI than Eq. (3.35), which misleadingly overestimates the precision limit.

Finally, I discuss why the QCRB of the single-parameter estimation with the phase-averaging and the two-parameter estimation coincide when one of the inputs is vacuum. Let $\rho = \hat{\rho}^A_{\rm in} \otimes |0\rangle\langle 0|^B$ and consider its phase averaging. Then one observes,

$$\begin{aligned}
\Psi^{\rm OPA}_{\rm avg} &= \int \frac{d\theta}{2\pi} \hat{T}^{AB}_{\rm OPA} \hat{V}^A_\theta \hat{V}^B_\theta \hat{\rho} \hat{V}^{A\,\dagger}_\theta \hat{V}^{B\,\dagger}_\theta \hat{T}^{\dagger AB}_{\rm OPA} \\
&= \int \frac{d\theta}{2\pi} \hat{T}^{AB}_{\rm OPA} \hat{V}^A_\theta \hat{V}^B_{-\theta} \hat{\rho} \hat{V}^{A\,\dagger}_\theta \hat{V}^{B\,\dagger}_{-\theta} \hat{T}^{\dagger AB}_{\rm OPA} \\
&= \int \frac{d\theta}{2\pi} \hat{V}^A_\theta \hat{V}^B_{-\theta} \hat{T}^{AB}_{\rm OPA} \hat{\rho} \hat{T}^{\dagger AB}_{\rm OPA} \hat{V}^{A\,\dagger}_\theta \hat{V}^{B\,\dagger}_{-\theta},
\end{aligned} \tag{3.36}$$

where the second equality follows from the fact that the phase shift does not change the

vacuum state and the third equality holds since the two-mode squeezing (OPA) operation commutes with the phase shift $\hat{V}_\theta^A \hat{V}_{-\theta}^B$. This shows that the phase averaging is effectively equivalent to adding another unknown phase θ in upper arm (mode A) and unknown phase $-\theta$ in lower arm (mode B). That is, the interferometer's phase difference is set to be unknown and thus the problem is equivalent to the estimation of two unknown parameters, ϕ_s and $\phi_d = 2\theta$ [41]. This results in the same precision bound for these two different problems. Note that the above only holds when one of the inputs is a vacuum but may not hold for more general inputs.

3.5 Non-vacuum Inputs for SU(1,1) Interferometer

3.5.1 Two coherent states

In this section, I generalize the above results for SU (1,1) Interferometer such that both inputs are non-vacuum. I consider the two-parameter estimation, i.e. ϕ_s and ϕ_d are both assumed to be unknown. For simplicity, I assume $\theta = 0$. When the input state is a tensor of two coherent states, $|\alpha\rangle_A \otimes |\beta\rangle_B$, where α and β are both complex, following the QFIM approach in the previous section, one gets

$$\Delta^2 \phi_s \geq F_{\text{coh}}^{-1}, \tag{3.37}$$

where

$$\begin{aligned} F_{\text{coh}} = &\frac{n_{\text{in}}^2 n_\kappa (n_\kappa + 2) + 4 n_a n_b (n_\kappa + 1)^2}{n_{\text{in}}} \\ &+ n_\kappa (n_\kappa + 2) + 2\text{Re}(\alpha\beta)\sinh(4g), \end{aligned} \tag{3.38}$$

and $n_{\text{in}} = |\alpha|^2 + |\beta|^2$. If $|\alpha|^2 = 0$ or $|\beta|^2 = 0$, one gets back Eq. (3.20). Note that Eq. (3.38) is always tighter than the one in Ref. [27]. This discrepancy comes from the fact that Ref. [27] treated the problem effectively as a single-parameter estimation (i.e. implicitly assuming that ϕ_d is known a priori). Also, when $n_\kappa = 0$, and there is no OPA, then the

two arms never interact before the measurement step, and one gets

$$F_{\text{coh}}^{n_\kappa \to 0} = \frac{4\left|\alpha\right|^2\left|\beta\right|^2}{\left|\alpha\right|^2+\left|\beta\right|^2}. \tag{3.39}$$

This result matches with the "one-mode" interferometer model described in Ref. [41].

For given n_κ and n_{in}, F_{coh} is maximized when two inputs have the same amplitude and conjugate phase, i.e. $\alpha = |\alpha|e^{i\varphi}$ and $\beta = |\beta|e^{-i\varphi}$ with $|\alpha| = |\beta|$. Then Eq. (3.38) reduces to be

$$\begin{aligned} F_{\text{coh}}^{\max} &= (n_{\text{in}}+1)n_\kappa(n_\kappa+2) + n_{\text{in}}(n_\kappa+1)^2 \\ &+ 4n_{\text{in}}\sqrt{n_\kappa(n_\kappa+1)}(2n_\kappa+1), \end{aligned} \tag{3.40}$$

where note that $\sinh(4g) = 4\sqrt{n_\kappa(n_\kappa+1)}(2n_\kappa+1)$. One observes that $F_{\text{coh}}^{\max}$ is basically proportional to n_κ^2 and n_{in}. Thus, if one restricts only the total input power to the system $n_{\text{tot}} = n_\kappa + n_{\text{in}}$, it suggests one should concentrate all power to the parametric gain to maximize the quantum advantage beyond the shot noise limit. If instead one has a restriction on n_κ due to practical reasons, the coherent state input still can boost the sensitivity by a factor proportional to n_{in}.

3.5.2 Coherent state and squeezed vacuum

I further extend the analysis for the input of coherent state and squeezed vacuum: $|\alpha\rangle_A \otimes |\xi\rangle_B$. For simplicity, one assumes α is real. By using QFIM method, one gets the estimation of the phase sum ϕ_s as in Eq. (3.31), is bounded by the QFI:

$$\begin{aligned} F_Q^1 &= \sinh^2(2g)\left[\left|\alpha\right|^2 \mathrm{e}^{2r} + \cosh^2(r)\right] \\ &+ \cosh^2(2g)\frac{8\left|\alpha\right|^2\sinh^2(2r)}{4\left|\alpha\right|^2 + 2\sinh^2(2r)}, \end{aligned} \tag{3.41}$$

where r is the squeezing strength of the squeezed vacuum $|\xi\rangle$. When any or both of the input state is vacuum, i.e, $r = 0$ or $|\alpha|^2 = 0$, one gets back Eq. (3.20). In addition, when $g = 0$, this means that the two modes don't interact before the measurement step, and when either $r = 0$ or $|\alpha|^2 = 0$, one gets $F = 0$, which is consistent with our intuition.

It is worthwhile to compare the above result with that of Li *et al.*'s. The QFI in Ref. [26] is given by:

$$\begin{aligned} F_Q^2 = &\sinh^2(2g)\left[|\alpha|^2 \mathrm{e}^{2r} + \cosh^2(r)\right] \\ &+ \cosh^2(2g)\left[|\alpha|^2 + \frac{1}{2}\sinh^2(2r)\right]. \end{aligned} \tag{3.42}$$

The difference between F_Q^1 and F_Q^2 is given by:

$$F_Q^1 - F_Q^2 = -\cosh^2 2g \frac{\left[-4|\alpha|^2 + \cosh(4r) - 1\right]^2}{4\left[4|\alpha|^2 + \cosh(4r) - 1\right]}, \tag{3.43}$$

One can see the difference is always negative, which suggests that our phase sensitivity,given by F_Q^1, provides a tighter QCRB.

It is also interesting to compare the bound in Eq. (3.41) with the classical Fisher information (CFI) of parity detection, which is the known best strategy in ideal scenario in this setup [26]. The CFI of parity detection is given by

$$F_{\mathrm{cl}} = \sinh^2(2g)\left[|\alpha|^2 \mathrm{e}^{2r} + \cosh^2(r)\right]. \tag{3.44}$$

Obviously, F_Q^1 is larger than F_{cl}, which suggests that the parity measurement is indeed not the optimal measurement in this case. Note that for multi-parameter estimation problems, there is no guarantee that there exists a set of POVM which saturates the QCRB [15, 42, 43, 44, 45].

3.6 Summary

In this chapter, I revisited the quantum Fisher information approach to establish a fundamental precision estimation bounds for Mach-Zehnder and SU(1,1) interferometers. For MZI, firstly, if both arms of the MZI have different unknown phase shifts in the application and the input to one of the two ports is vacuum, then no matter what the input in the other port is, and no matter the detection scheme, one can never better the SNL in phase sensitivity. This statement holds even if the first beamsplitter of the MZI is non-50:50. The proof is based on the fact that it is intrinsically a two-parameter estimation problem. That is, one cannot ignore the phase sum ϕ_s in the analysis though it is often treated as a "global phase" and ignored in real experiments. This type of sensing includes gravitational wave detection [16, 17], long-baseline interferometry [46], and differential interference contrast microscopy [47, 48], for example. In these applications, if one input is vacuum, our result rules out the possibility of doing something "quantum" at the detector (such as putting in a squeezer or doing photon addition or subtraction) to beat the SNL.

Secondly, if only one of the MZI arms has an unknown phase shift in the application, then the ultimate precision limit depends on the detector restriction. If one does not allow the detector to use any external phase reference and power resource, then the precision is limited by the SNL. However, if the detector is allowed to use such resources, then one can beat the SNL in terms of the total resource used at the input and detector. The explicit sensing scheme which uses squeezers for both input and detector is given. This type of sensing includes simple MZI devices measuring sample's density, pressure, temperature, etc, and also LIDAR-type sensing [49]. In these applications, only if nonclassical light is introduced into at least one input port, is there a hope to beat the SNL by doing something quantum at the detector, even if the other port is vacuum.

For SU(1,1) interferometer, firstly, when one of the input states is restricted to be a vacuum state, I showed that by using either the phase-averaging method or the quantum Fisher information matrix method, different phase configurations of the SU(1,1) interfer-

ometer result in the same QFI. In this case, the QFI is linearly proportional to the average photon number of the second input state, and quadratically proportional to the average photon number generated by the OPA. This suggests that when fixing the squeezing strength of the OPA, to achieve higher sensitivity, one simply needs to inject a state with higher average photon number. Secondly, I compared the results of the phase-averaging method and the quantum Fisher information matrix method, and then I argued that for a SU(1,1) interferometer, phase averaging or quantum Fisher information matrix method is generally required, and they are essentially equivalent. Finally, I used the quantum Fisher information matrix method to calculate the precision limit for other common input states, such as two coherent state inputs or coherent state with squeezed vacuum inputs.

Chapter 4
Multiparameter Estimation with Single Photons

4.1 Introduction

Phase parameter estimation with optical interferometry has long been a cornerstone for studying systems of both theoretical and practical interest, even as early as the Michelson-Morley experiment in 1887. Since the discovery of quantum optical interferometry, it has been shown that strategies utilizing non-classical states of light can be used for both single and multiple parameter estimation to theoretically allow for advantages in precision over classical methods [50, 51, 52, 10, 53, 7, 54, 55]. These quantum advantages are of particular interest for applications where the target is especially photosensitive, such as in the imaging of biological tissue, where estimating multiple parameters simultaneously is a fundamental task [56, 57, 58, 59, 60]. Unfortunately, many of the quantum states required to enable these strategies are notoriously difficult to create or are extremely sensitive to noise, therefore limiting the systems of interest in which quantum optical interferometry might be realistically advantageous [61, 62, 35, 63, 64, 49, 11, 65]. The search continues to find architectures and states, which can achieve some level of super-sensitivity (beating the equivalent of the shotnoise limit), but can be readily made and are robust to noise[1].

Meanwhile, experimental BosonSampling is claimed to be a leading candidate for showing post-classical computation [66, 67, 68, 69, 70, 71, 72, 73]. This has been a major motivating factor for a renewed interest in linear optical systems, although the claims for demonstrating imminent quantum supremacy is still under debate [74, 75]. Much of the interest in BosonSampling arises due to the great progress on the development and improvement of single-photon sources [76, 77, 78, 79, 80]. These sources, together with high-efficiency detectors and waveguides, which can be integrated onto an all-optical chip,

[1]This Chapter is based on the contents of: C You, S Adhikari, Y Chi, M L LaBorde, C T Matyas, C Zhang, Z Su, T Byrnes, C Lu, J P Dowling and J P Olson. Multiparameter estimation with single photons–linearly–optically generated quantum entanglement beats the shot-noise limit. Journal of Optics, 19, 124002, 2017. Reprinted by permission of IOP Publishing. https://publishingsupport.iopscience.iop.org/questions/rp-use-of-a-subscription-article-in-your-thesis-or-dissertation-may-i-include-the-final-published-version-of-the-article-in-my-research-thesis-or-dissertation/

allow for an impressive level of fidelity in comparison to networks utilizing nonlinear optical elements and photon-number resolving detectors that are often necessary for implementing quantum metrology architectures. It was recently shown in Refs. [81, 82] that multimode interferometric devices comprised of only these simple linear components, including quantum Fourier transform interferometers (QUFTI), can be used to achieve super-sensitivity for single parameter estimation. Moreover, a recent experiment has further proved the quantum advantage of these purposed schemes [83]. A similar device with photon-number resolving measurements was shown to be supersensitive for multiparameter estimation [50]. In each case, however, the maximum number of modes which admitted an improvement over the shotnoise limit was small.

In this chapter, I consider an analogous architecture that admits super-sensitivity for multi-parameter estimation while maintaining a relatively modest experimental overhead. Our analytic computation of the Fisher information for our device (Fig. 4.1) shows that the sensitivity continues to beat the shotnoise limit—even in the limit of a large number of modes. Additionally, I show that our designs scale surprisingly well under photon loss and non-deterministic photon production from a source.

4.2 Multi-parameter Estimation in a Parallel QuFTI

In this current section I consider an architecture for an interferometer similar to our single parameter estimation strategy originally described in Ref. [82], where instead I now consider an estimate of multiple independent phases simultaneously. The interferometer consists of m mode with a photon in each mode with input $|\psi_{\text{in}}\rangle = |1\rangle^{\otimes m}$, as shown in Fig. 4.1. The input is fed into a particular passive linear optical unitary $\hat{U} = \hat{V}\hat{\Phi}\hat{V}^{\dagger}$, where $\hat{V} = \{V_{ij}\}$ is the quantum Fourier transform

$$V_{ij} = \frac{1}{\sqrt{m}} e^{2\pi(i-1)(j-1)/m}, \tag{4.1}$$

and $\hat{\Phi} = \{\Phi_{k\ell}\}$ is a $m \times m$ diagonal matrix of d independent phases $\vec{\boldsymbol{\varphi}} = \{\varphi_j\}_{j=1}^{d}$ which one would like to estimate. $\hat{\Phi}$ is diagonal and has the form,

$$\Phi_{k\ell} = \begin{cases} \delta_{k\ell} \cdot e^{i\varphi_k} & k \leq d \\ \delta_{k\ell} & k > d \end{cases} . \tag{4.2}$$

Other than the form of $\hat{\Phi}$, the above is identical to our previous QuFTI of Ref. [82], which leads us to refer to this device as a "parallel QuFTI". In Section 4.3, I will consider several different measurement strategies ranging from photon counting with number-resolution to on-off photodetection, which only distinguishes vacuum from a non-zero number of photons. For each strategy, the resulting probability distribution obtained from repeated measurements then acts as a measure of the unknown p hases.

The output state $|\psi_{\text{out}}\rangle$ of the interferometer is,

$$|\psi_{\text{out}}\rangle = \hat{U}|\psi_{\text{in}}\rangle = \sum_i \gamma^{(i)} |n_1^{(i)}, \ldots, n_m^{(i)}\rangle = \sum_i \gamma^{(i)} |\boldsymbol{n}^{(i)}\rangle, \tag{4.3}$$

where the sum is over all possible output photon configurations $|\boldsymbol{n}^{(i)}\rangle = |n_1^{(i)}, \ldots, n_m^{(i)}\rangle$ with m total photons, i.e. $\sum_j n_j^{(i)} = m$.

The coefficients $\gamma^{(i)}$ of every output configuration are related to matrix permanents of matrices closely related to $\hat{U}$ [84]. More precisely, for the photon configuration i and associated matrix permanent $\text{perm}(W^{(i)})$, if one denotes the jth row vector of $\hat{U}$ as $\mathbf{u}_j$, then $W^{(i)}$ consists of $n_j^{(i)}$ rows of $\mathbf{u}_j$ (note that matrix permanents are invariant under row interchange, so the ordering of the rows is unimportant). The corresponding coefficient is given by,

$$\gamma^{(i)} = \frac{\text{perm}(W^{(i)})}{\sqrt{n_1^{(i)}! \ldots n_m^{(i)}!}}. \tag{4.4}$$

Note that although the computational complexity of matrix permanents is in general $\#P$-hard to compute, even in the average case, matrices with certain symmetries may still be

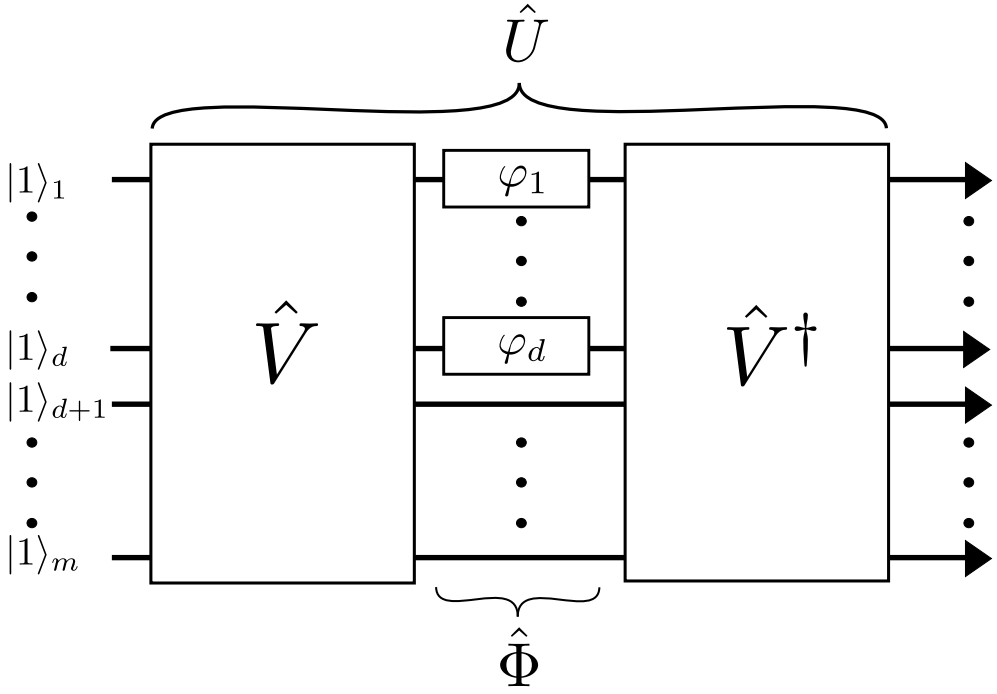

Figure 4.1: Architecture of the proposed parallel QuFTI optical interferometer, which simultaneously measures d independent unknown phases $\{\varphi_j\}_{j=1}^{d}$. The interferometer consists of m modes with an input of m single photons, $|1\rangle^{\otimes m}$. The unitary $\hat{V}$ (and its conjugate) is a quantum Fourier transform implemented with a network of beamsplitters and phase shifters. Several detection strategies for the output are presented in Section 4.3. For comparison, the architecture of the sequential QUMI is shown in Appendix G, Fig. G.1.

tractable, such as the configuration $|\boldsymbol{n}\rangle = |1, 1, \ldots, 1\rangle$ when $d = 1$ [81].

Recall that our goal is to use the interferometer described above to estimate the d unknown phases $\vec{\boldsymbol{\varphi}}$. For a given measurement scheme, the Cramér-Rao bound limits the precision of an estimate via the inequality,

$$|\Delta\vec{\boldsymbol{\varphi}}|^2 \equiv \sum_{j=1}^{d} \Delta\varphi_j^2 \equiv \mathrm{Tr}[\mathrm{Cov}(\vec{\boldsymbol{\varphi}})] \geq \frac{1}{\nu}\mathrm{Tr}[\mathcal{F}_{\vec{\boldsymbol{\varphi}}}^{-1}] \tag{4.5}$$

where ν is the number of independent trials, and the matrix $\mathcal{F}_{\vec{\boldsymbol{\varphi}}} = \{\mathcal{F}_{i,j}^{\mathrm{clas}}\}$ is the classical Fisher information given by,

$$\mathcal{F}_{i,j}^{\mathrm{clas}} = \sum_{x} \frac{1}{p(x|\vec{\boldsymbol{\varphi}})} \frac{\partial p(x|\vec{\boldsymbol{\varphi}})}{\partial\varphi_i} \frac{\partial p(x|\vec{\boldsymbol{\varphi}})}{\partial\varphi_j}, \tag{4.6}$$

where $p(x|\vec{\boldsymbol{\varphi}}) = |\langle x|\psi_{\text{out}}\rangle|^2$, which is the probability of observing outcome x conditioned on $\vec{\boldsymbol{\varphi}}$. Because of the dependence of the Fisher information on $\vec{\boldsymbol{\varphi}}$, it may be the case that the measurement precision is best near certain values of $\vec{\boldsymbol{\varphi}}$, as in Refs. [81, 85].

The quantum Cramér-Rao bound (QCRB) [15] lower-bounds the uncertainty of estimating $\vec{\boldsymbol{\varphi}}$ from a given *quantum* state that encodes information about $\vec{\boldsymbol{\varphi}}$, but is independent of any measurement scheme and dependent only on the probe state. The QCRB is identical to Eq. (4.5), except that the Fisher information matrix $\mathcal{F}^{\text{clas}}_{i,j}$ is replaced by the quantum Fisher information (QFI) matrix [15],

$$\mathcal{F}^{\text{quant}}_{i,j} = \frac{1}{2}\langle\psi_{\text{out}}|(L_i L_j + L_j L_i)|\psi_{\text{out}}\rangle. \tag{4.7}$$

where $L_i = 2(|\partial_{\varphi_i}\psi_{\text{out}}\rangle\langle\psi_{\text{out}}| + |\psi_{\text{out}}\rangle\langle\partial_{\varphi_i}\psi_{\text{out}}|)$. Subsequently, I will refer to $\mathcal{F}_{\vec{\boldsymbol{\varphi}}} = \{\mathcal{F}^{\text{quant}}_{i,j}\}$ to mean the QFI matrix. It is worth noting that the dimension of both the Fisher information matrix and the QFI matrix is equal to the number of phases one is estimating (d in our case).

It was shown by Humphreys et al. [50] that for arbitrary pure input states of multi-mode Fock states, the QFI matrix of the estimated phases is given as

$$\mathcal{F}_{\vec{\boldsymbol{\varphi}}} = 4\sum_i \left|\gamma^{(i)}\right|^2 |\boldsymbol{n}^{(i)}\rangle\langle\boldsymbol{n}^{(i)}| - 4\sum_{i,j}\left|\gamma^{(i)}\right|^2\left|\gamma^{(j)}\right|^2 |\boldsymbol{n}^{(i)}\rangle\langle\boldsymbol{n}^{(j)}|, \tag{4.8}$$

where the $\gamma^{(i)}$ are defined in Eq. (4.4). The quantum Fisher Information matrix can be calculated as,

$$[\mathcal{F}_{\vec{\boldsymbol{\varphi}}}]_{l,n} = 4\left\langle \hat{b}_l^\dagger \hat{b}_l \hat{b}_n^\dagger \hat{b}_n \right\rangle - 4\left\langle \hat{b}_l^\dagger \hat{b}_l \right\rangle \left\langle \hat{b}_n^\dagger \hat{b}_n \right\rangle, \tag{4.9}$$

where $\hat{b}_i^\dagger = \sum_j V_{i,j}\hat{a}_j^\dagger$ [86]. Calculating the QFI for the setup with a k-photon Fock state in

every mode, one obtains,

$$\mathcal{F}_{\vec{\varphi}} = 4k(k+1)\begin{pmatrix} \frac{m-1}{m} & -\frac{1}{m} & \cdots & -\frac{1}{m} \\ -\frac{1}{m} & \frac{m-1}{m} & \cdots & -\frac{1}{m} \\ \vdots & \vdots & \ddots & \vdots \\ -\frac{1}{m} & -\frac{1}{m} & \cdots & \frac{m-1}{m} \end{pmatrix}, \tag{4.10}$$

Details of the calculation can be found in Appendix F. Computing its inverse [87], one finds a similarly patterned matrix,

$$\mathcal{F}_{\vec{\varphi}}^{-1} = \frac{1}{4k(k+1)}\begin{pmatrix} \frac{m-d+1}{m-d} & \frac{1}{m-d} & \cdots & \frac{1}{m-d} \\ \frac{1}{m-d} & \frac{m-d+1}{m-d} & \cdots & \frac{1}{m-d} \\ \vdots & \vdots & \ddots & \vdots \\ \frac{1}{m-d} & \frac{1}{m-d} & \cdots & \frac{m-d+1}{m-d} \end{pmatrix}. \tag{4.11}$$

Substituting the trace of $\mathcal{F}_{\vec{\varphi}}^{-1}$ into Eq. (4.5) and recalling the matrix is $d \times d$, one arrives at the bound,

$$|\Delta\vec{\varphi}|^2 \geq \frac{1}{\nu}\frac{1}{4k(k+1)}\frac{d(m-d+1)}{(m-d)}. \tag{4.12}$$

In this chapter, I will consider the case that $k = 1$, since on-demand single-photon sources are quickly becoming experimentally viable. While larger Fock state generation remains a challenge [88], it is interesting to see that, since $|\Delta\vec{\varphi}|^2$ scales inversely with k^2, indicating that an asymptotic improvement approaching the Heisenberg limit is possible if such states could be easily prepared.

4.3 Measurement Strategies

To examine the sensitivity of the described multi-arm interferometer, I will first compare the QFI for several different phase estimation strategies, assuming that the QCRB can be saturated in each case. Suppose there are m modes, and I wish to simultaneously measure d phases, where $d < m$ (at least one arm must be used as a reference). For $k = 1$,

Eq. (4.12) reduces to,

$$|\Delta\vec{\boldsymbol{\varphi}}_1|^2 = \frac{1}{\nu_1}\frac{(m-d+1)d}{8(m-d)}, \tag{4.13}$$

where ν_1 denotes the number of measurements for the parallel QuFTI.

To show any advantage for our scheme, one must compare our setup to other relevant architectures, which are limited in the same resources. One may consider a strategy using an identical interferometer, except where only a single phase is estimated at a time. Such a strategy is simply a sequential version of the scheme developed by Olson et al. [81]. I will refer this comparator scheme as "sequential QUMI" for the remainder of this chapter. Another comparison is made to the classical strategy where the inputs are uncorrelated coherent states $\otimes_{i=1}^{m}|\alpha_i\rangle$.

To make a fair comparison, I will restrict that these three different schemes should use the same amount of photons. For the sequential QUMI, since one have d phases to measure, and one needs at least m photons for a measurement of each phase, the variance becomes,

$$|\Delta\vec{\boldsymbol{\varphi}}_2|^2 = \frac{1}{\nu_2}\left(\frac{1}{\sqrt{8\left(1-\frac{1}{m}\right)}}\right)^2 d = \frac{1}{\nu_2}\frac{md}{8\,(m-1)}, \tag{4.14}$$

where ν_2 is the number of repetitions of this protocol, and I have used the result of Ref. [81] to compute the sensitivity. For $\nu_2 = 1$, the total number of photons used in sequential QUMI measurement is md.

For the parallel QuFTI, a single measurement requires m photons. Thus, for a fair comparison against the sequential QUMI, one requires $\nu_1 = d\nu_2$ so that Eq. (4.13) becomes,

$$|\Delta\vec{\boldsymbol{\varphi}}_1|^2 = \frac{1}{\nu_1}\frac{(m-d+1)d}{8(m-d)} = \frac{1}{\nu_2}\frac{(m-d+1)}{8(m-d)}. \tag{4.15}$$

Finally, for the classical strategy, I let the average photon number of the input $\bar{n} =$

$\sum_{i=1}^{m} |\alpha_i|^2 = md$ so that a fair comparison requires $\nu_3 = \nu_2$, and the variance is [50],

$$|\Delta\vec{\varphi}_3|^2 = \frac{1}{\nu_3}\frac{d^2}{md} = \frac{1}{\nu_2}\frac{d}{m}. \tag{4.16}$$

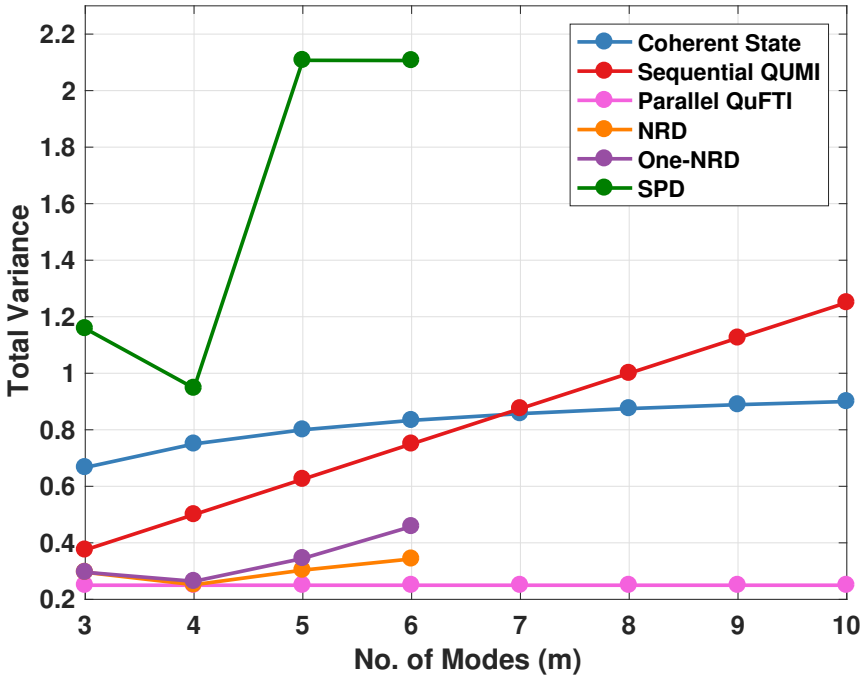

Figure 4.2: Total variance ($\Delta\vec{\varphi}^2$) with different metrological strategies when estimating multiple ($d = m - 1$) parameters. The QCRB for the parallel QuFTI strategy (pink, Eq. 4.13) gives the lowerbound on the variance for any measurement scheme. The One-NRD (purple), SPD (green) and NRD (orange) are obtained from numerically optimizing $\boldsymbol{\varphi}$ from the classical CRB (Eq. 4.5). For comparison, the coherent state strategy (blue, Eq. 4.16) and sequential QUMI (red, Eq. 4.14) are shown.

Now that the variance of each strategy is expressed in terms of the same number of photons (namely, $md\nu_2$), one can easily compare them. In the case that $d = 1$, the sequential QUMI and parallel QuFTI are identical strategies, and the comparison against the classical strategy mirrors the prior result from Ref. [81], which showed an improvement over the classical strategy only for $m < 7$. However, as one scales up d along with m, one sees that the parallel QuFTI, the scheme I propose in this chapter, continues to improve relative to the classical strategy. Indeed, setting $d = m - 1$ yields the maximum improvement over the

classical case, where our parallel QuFTI achieves an asymptotic improvement of a factor of four in the total variance (see Fig. 4.2).

However, one should provide an actual detection scheme, rather than only providing a QFI calculation alone, to make a useful comparison. This is because, while the QFI gives a theoretically attainable bound on the sensitivity, one wishes to consider detection schemes, which can be realistically implemented [32]. For the sequential QUMI and coherent state strategies, single-photon detectors (SPD) and homodyne detection make up the QCRB-saturating measurement schemes, respectively. For the parallel QuFTI, I will consider several cases. Note that to compute the sensitivity of these specific detection schemes, I numerically compute the minimum of the classical Fisher information $\mathcal{F}^{\text{clas}}$ corresponding to these schemes. However, numerically computing these values for a large number of modes was problematic due to the complex landscape optimization of the Fisher information. In addition to the overhead of calculating the matrix permanents, the optimization showed a sensitive dependence to the phases making it a numerically intensive task.

First, one sees that a detection scheme corresponding to an array of m photon number-resolving detectors (NRDs) nearly achieves the QCRB of our parallel QuFTI (for values I was able to compute). There exists high-efficiency NRDs, which could be either implemented by tungsten transition edge sensor [89] or titanium-based transition edge sensors [90]. However, NRDs are known to be far more costly and difficult to implement experimentally than SPDs. Moreover, the current NRD has a low counting rate [91]. While an array of SPDs performed well for QUMI (single phase estimation), SPDs unfortunately perform quite poorly for estimating multiple phases simultaneously even for small m.

To bridge the gap between these two measurement schemes, I propose a new measurement scheme which is far less experimentally demanding. I consider a combination of a single NRD in one arm together with SPDs in the remaining arms. Using this scheme, I note a sensitivity at par with the NRD case for small numbers of modes. One can see why this may be the case for a small number of modes—because of the symmetry of the QFT,

regardless of the phases, any cyclic permutation of event outcomes are equally likely (for instance, if $m = 3$, the (1,2,0), (0,1,2) and (2,0,1) outcomes occur with the same frequency). Of course, with the increase in the number of modes, the number of distinguishable events reduces, and one expects the sensitivity to worsen if one do not include more NRDs. Furthermore, the presence of a single NRD can be approximated experimentally by mixing the target mode with a series of vacuum modes using beamsplitters, and placing SPDs at the output of each of these modes, as was done in Ref. [92].

4.4 Probabilistic Photon Sources

The parallel QuFTI, particularly for a small number of modes with few NRDs, is readily implementable in a laboratory with available technology. One of the main requirements needed for our scheme is the generation of indistinguishable photons. There have been many proposals for single photon sources using atoms [93], molecules [94], color centers in diamond [95], quantum dots [73, 96], and spontaneous parametric down conversion (SPDC) [85]. Because many of these techniques produce single photons probabilistically, an input state consisting of m photons is not always guaranteed.

Although it may be expected that truly on-demand sources will be available in the near future, I nonetheless consider a "scattershot" input state to take into account the probabilistic nature of photon generation. A similar approach was recently proposed and demonstrated to improve the sampling efficiency for BosonSampling [85, 97]. In an analogous way, I show that our scheme can still provide a sub-shotnoise sensitivity even when the photon sources are not necessarily reliable on-demand sources.

In a scattershot scenario, photon pairs are emitted from a source (for instance, a SPDC) with some non-unit probability. A detection event of the one photon heralds the injection of the twin photon into a specific port of the interferometer. In this way, at a given time, one can keep track of the modes which received an input photon and the total number of photons present inside the interferometer. With knowledge of the input, one can still make inferences about the phase, albeit with a lower sensitivity than an input with a full array

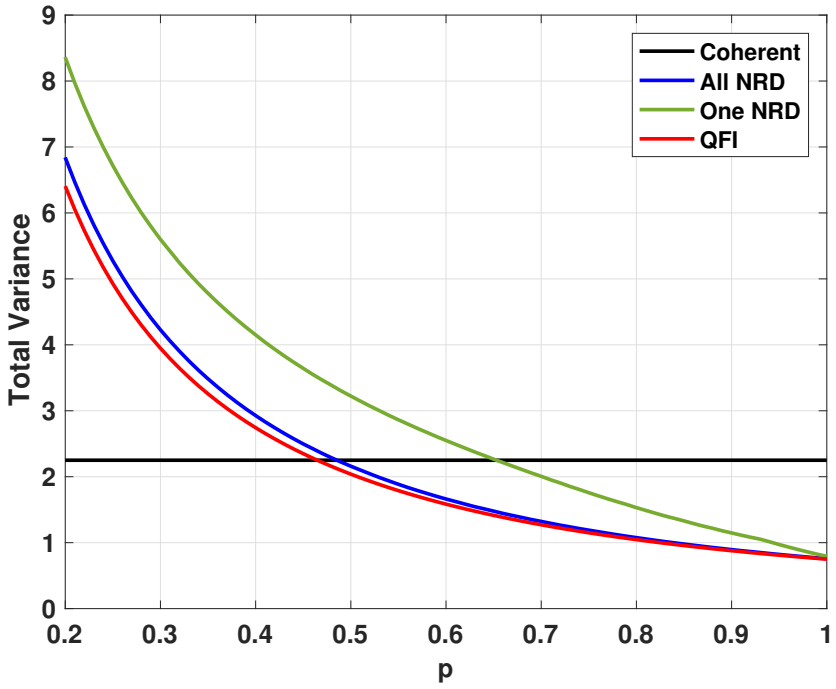

Figure 4.3: Total variance ($\Delta\vec{\varphi}^2_{\text{avg}}$) for scattershot four-mode, three-phase parallel QuFTI using all NRD detection scheme (blue line) and one-NRD detection scheme (green line) with photon source efficiency p compared to the minimum variance for a lossless coherent source (black) with average photon number $\bar{n} = 4$.

of m deterministic photon sources.

Consider a source of m SPDC where the probability of generating a particular input configuration is p_i. For each input configuration, one can compute the associated variance $\Delta\vec{\varphi}^2_i$ from the classical Fisher information, so that the average variance $\Delta\vec{\varphi}^2_{\text{avg}}$ is given by,

$$\Delta\vec{\varphi}^{-2}_{\text{avg}} = \sum_{i=1} p_i \Delta\vec{\varphi}^{-2}_i, \tag{4.17}$$

where the summation is over the total number of input configurations.

I numerically consider the case of a four-mode, three-phase parallel QuFTI with probabilistic photon sources, where for simplicity all sources have an equal probability p of emitting a heralded photon. As one can see in Fig. 4.3, even for a source efficiency around 50%, one can still beat a lossless coherent source, if one possesses a full NRD measurement.

Yet even for a single NRD, a source of 65% efficiency can still achieve supersensitivity.

4.5 Summary

In this chapter, I have considered a passive multi-mode interferometer for multiparameter phase estimation. I have shown that the quantum Cramér-Rao bound admits an asymptotic constant factor improvement in the sensitivity by a factor of 4, which can be approximately obtained for a small number of modes with an array of single photon detectors and only one number-resolving detector. Remarkably, supersensitivity can be observed even with inefficient but heralded single photon sources.

As the number of modes increases, one expects that a single NRD will be insufficient to capture the required information that allows the device to be supersensitive. A future analysis of the scaling of the number of NRDs necessary to maintain supersensitivity would be useful to determine if this device would then imply a truly scalable quantum measurement device that exceeds the precision of classical sensors.

Chapter 5
Conclusion

In this dissertation, I discussed several topics in the field of quantum metrology. The basics of the quantum state of light and quantum metrology are reviewed and discussed. In Chapter 3, I revisited the quantum Fisher information approach to the two-mode interferometer. More specifically, I considered the Mach-Zehnder interferometer and SU(1,1) interferometer. I tried to establish a fundamental precision estimation bound for such a device, motivated by the fact that many previous works in this field fail to accurately count the resources used in the interferometers. For the MZI, one can never do better than the SNL in phase sensitivity, when the input to one of the two ports is the vacuum. If one does not allow the detector to use any external phase reference and power resource, then the precision is limited by the SNL. For the SU(1,1) interferometer, first, when one of the input states is restricted to be a vacuum state, I showed that by using either the phase-averaging method or the quantum Fisher information matrix method, different phase configurations of the SU(1,1) interferometer result in the same QFI. Second, I compared the results of the phase-averaging method and the quantum Fisher information matrix method, and found that for an SU(1,1) interferometer, phase averaging or quantum Fisher information matrix method is generally required, and they are essentially equivalent. Finally, I used the quantum Fisher information matrix method to calculate the precision limit for other common input states, such as two-coherent-state inputs or coherent state with squeezed vacuum inputs.

In Chapter 4, I considered a passive multi-mode interferometer for multiparameter phase estimation. I have shown that the quantum Cramér-Rao bound admits an asymptotic constant factor improvement in the sensitivity by a factor of 4, which can be approximately obtained for a small number of modes with an array of single photon detectors and only one number-resolving detector. Remarkably, supersensitivity can be observed even with inefficient but heralded single photon sources.

References

[1] Yang Gao, Petr M. Anisimov, Christoph F. Wildfeuer, Jerome Luine, Hwang Lee, and Jonathan P. Dowling. Super-resolution at the shot-noise limit with coherent states and photon-number-resolving detectors. *J. Opt. Soc. Am. B*, 27(6):A170–A174, Jun 2010.

[2] Kebei Jiang, Hwang Lee, Christopher C. Gerry, and Jonathan P. Dowling. Super-resolving quantum radar: Coherent-state sources with homodyne detection suffice to beat the diffraction limit. *J. Appl. Phys*, 114(19), 2013.

[3] P. Kok, A. N. Boto, D. S. Abrams, C. P. Williams, S. L. Braunstein, and J. P. Dowling. Quantum-interferometric optical lithography: Towards arbitrary two-dimensional patterns. *Phys. Rev. A*, 63:063407, May 2001.

[4] P. Kok, S. L. Braunstein, and J. P. Dowling. Quantum lithography, entanglement and heisenberg-limited parameter estimation. *J. Opt. B: Quantum Semiclass. Opt.*, 6(8):S811, 2004.

[5] B. P. Abbott, R. Abbott, T. D. Abbott, and et al. Observation of gravitational waves from a binary black hole merger. *Phys. Rev. Lett.*, 116:061102, Feb 2016.

[6] B. P. Abbott, R. Abbott, T. D. Abbott, and et al. Gw151226: Observation of gravitational waves from a 22-solar-mass binary black hole coalescence. *Phys. Rev. Lett.*, 116:241103, Jun 2016.

[7] Vittorio Giovannetti, Seth Lloyd, and Lorenzo Maccone. Quantum metrology. *Phys. Rev. Lett.*, 96:010401, 2006.

[8] Carlton M. Caves. Quantum-mechanical noise in an interferometer. *Phys. Rev. D*, 23:1693–1708, Apr 1981.

[9] Agedi N. Boto, Pieter Kok, Daniel S. Abrams, Samuel L. Braunstein, Colin P. Williams, and Jonathan P. Dowling. Quantum interferometric optical lithography: Exploiting entanglement to beat the diffraction limit. *Phys. Rev. Lett.*, 85:2733–2736, Sep 2000.

[10] Jonathan P. Dowling. Quantum optical metrology – the lowdown on high-n00n states. *Contemp. Phys.*, 49(2):125–143, 2008.

[11] Petr M. Anisimov, Gretchen M. Raterman, Aravind Chiruvelli, William N. Plick, Sean D. Huver, Hwang Lee, and Jonathan P. Dowling. Quantum metrology with two-mode squeezed vacuum: Parity detection beats the heisenberg limit. *Phys. Rev. Lett.*, 104:103602, 2010.

[12] Bernard Yurke, Samuel L. McCall, and John R. Klauder. SU(2) and SU(1,1) interferometers. *Phys. Rev. A*, 33:4033–4054, Jun 1986.

[13] Steven M Kay. Fundamentals of statistical signal processing, volume 1 of. *Signal Processing*, 1993.

[14] Samuel L. Braunstein and Carlton M. Caves. Statistical distance and the geometry of quantum states. *Phys. Rev. Lett.*, 72:3439–3443, May 1994.

[15] C. W. Helstrom. *Quantum Detection and Estimation Theory.* Academic Press, New York, 1976.

[16] H. Grote, K. Danzmann, K. L. Dooley, R. Schnabel, J. Slutsky, and H. Vahlbruch. First long-term application of squeezed states of light in a gravitational-wave observatory. *Phys. Rev. Lett.*, 110:181101, May 2013.

[17] L. A. Lugiato, A. Gatti, and E. Brambilla. Quantum imaging. *J. Opt. B: Quantum Semiclass. Opt.*, 4(3):S176, 2002.

[18] Luca Pezzé and Augusto Smerzi. Ultrasensitive two-mode interferometry with single-mode number squeezing. *Phys. Rev. Lett.*, 110(16):163604, 2013.

[19] Matthias D. Lang and Carlton M. Caves. Optimal quantum-enhanced interferometry using a laser power source. *Phys. Rev. Lett.*, 111:173601, Oct 2013.

[20] Jing Liu, Xiaoxing Jing, and Xiaoguang Wang. Phase-matching condition for enhancement of phase sensitivity in quantum metrology. *Phys. Rev. A*, 88(4):042316, 2013.

[21] Marcin Jarzyna and Rafał Demkowicz-Dobrzański. Quantum interferometry with and without an external phase reference. *Phys. Rev. A*, 85:011801, Jan 2012.

[22] Luca Pezzè, Philipp Hyllus, and Augusto Smerzi. Phase-sensitivity bounds for two-mode interferometers. *Phys. Rev. A*, 91:032103, Mar 2015.

[23] William N. Plick, Jonathan P. Dowling, and Girish S. Agarwal. Coherent-light-boosted, sub-shot noise, quantum interferometry. *New J. Phys.*, 12(8):083014, 2010.

[24] Z. Y. Ou. Enhancement of the phase-measurement sensitivity beyond the standard quantum limit by a nonlinear interferometer. *Phys. Rev. A*, 85:023815, Feb 2012.

[25] Dong Li, Chun-Hua Yuan, Z Y Ou, and Weiping Zhang. The phase sensitivity of an su (1, 1) interferometer with coherent and squeezed-vacuum light. *New J. Phys.*, 16(7):073020, 2014.

[26] Dong Li, Bryan T. Gard, Yang Gao, Chun-Hua Yuan, Weiping Zhang, Hwang Lee, and Jonathan P. Dowling. Phase sensitivity at the heisenberg limit in an SU(1,1) interferometer via parity detection. *Phys. Rev. A*, 94:063840, Dec 2016.

[27] Chun-Hua Yuan Ze-Yu Ou Qian-Kun Gong, Dong Li and Wei-Ping Zhang. Bounds to precision for an SU(1,1) interferometer with gaussian input states. *Chinese Phys. B*, 26, 2017.

[28] Brian E. Anderson, Bonnie L. Schmittberger, Prasoon Gupta, Kevin M. Jones, and Paul D. Lett. Optimal phase measurements with bright- and vacuum-seeded SU(1,1) interferometers. *Phys. Rev. A*, 95:063843, Jun 2017.

[29] Brian E. Anderson, Prasoon Gupta, Bonnie L. Schmittberger, Travis Horrom, Carla Hermann-Avigliano, Kevin M. Jones, and Paul D. Lett. Phase sensing beyond the standard quantum limit with a variation on the SU(1,1) interferometer. *Optica*, 4:752–756, July 2017.

[30] Stuart S. Szigeti, Robert J. Lewis-Swan, and Simon A. Haine. Pumped-up SU(1,1) interferometry. *Phys. Rev. Lett.*, 118:150401, Apr 2017.

[31] Jian-Dong Zhang, Chen-Fei Jin, Zi-Jing Zhang, Long-Zhu Cen, Jun-Yan Hu, and Yuan Zhao. Super-sensitive angular displacement estimation via an SU(1,1)-SU(2) hybrid interferometer. *Opt. Express*, 26(25):33080–33090, Dec 2018.

[32] Masahiro Takeoka, Kaushik P. Seshadreesan, Chenglong You, Shuro Izumi, and Jonathan P. Dowling. Fundamental precision limit of a Mach-Zehnder interferometric sensor when one of the inputs is the vacuum. *Phys. Rev. A*, 96:052118, Nov 2017.

[33] G. S. Agarwal. *Quantum Optics*. Cambridge, 2013.

[34] Akio Fujiwara and Hiroshi Imai. A fibre bundle over manifolds of quantum channels and its application to quantum statistics. *J. Phys. A*, 41(25):255304, 2008.

[35] Rafal Demkowicz-Dobrzański, Marcin Jarzyna, and Jan Kołodyński. Chapter four - quantum limits in optical interferometry. volume 60 of *Progress in Optics*, pages 345 – 435. Elsevier, 2015.

[36] Denes Petz. Monotone metrics on matrix spaces. *Linear Algebra and Its Applications*, 244(1996):81–96, 1996.

[37] Denes Petz and Catalin Ghinea. *Introduction to quantum Fisher Information*, pages 261–281.

[38] Akio Fujiwara. Quantum channel identification problem. *Phys. Rev. A*, 63:042304, Mar 2001.

[39] Chenglong You, Sushovit Adhikari, Yuxi Chi, Margarite L LaBorde, Corey T Matyas, Chenyu Zhang, Zuen Su, Tim Byrnes, Chaoyang Lu, Jonathan P Dowling, et al. Multiparameter estimation with single photons—linearly-optically generated quantum entanglement beats the shotnoise limit. *J. Opt.*, 19(12):124002, 2017.

[40] Matthias D. Lang and Carlton M. Caves. Optimal quantum-enhanced interferometry. *Phys. Rev. A*, 90:025802, Aug 2014.

[41] Marcin Jarzyna. PhD dissertation, University of Warsaw, 2016.

[42] Keiji Matsumoto. A new approach to the cramér-rao-type bound of the pure-state model. *J. Phys. A: Math. Gen.*, 35(13):3111, 2002.

[43] Sammy Ragy, Marcin Jarzyna, and Rafał Demkowicz-Dobrzański. Compatibility in multiparameter quantum metrology. *Phys. Rev. A*, 94:052108, Nov 2016.

[44] Luca Pezzè, Mario A. Ciampini, Nicolò Spagnolo, Peter C. Humphreys, Animesh Datta, Ian A. Walmsley, Marco Barbieri, Fabio Sciarrino, and Augusto Smerzi. Optimal measurements for simultaneous quantum estimation of multiple phases. *Phys. Rev. Lett.*, 119:130504, Sep 2017.

[45] Jing Yang, Shengshi Pang, Yiyu Zhou, and Andrew N Jordan. Optimal measurements for quantum multi-parameter estimation with general states. *arXiv preprint arXiv:1806.07337*, 2018.

[46] David Gerwe-Paul Idell Bryan Gard Richard Birrittella S M Hashemi Rafsanjani Mohammad Mirhosseini O S Magan-Loiza Jonathan Dowling Christofer Gerry Robert Boyd Barbara Capron Claudio Parazzoli, Benjamin Koltenbah. Enhanced thermal object imaging by photon addition or subtraction. *arXiv preprint arXiv:1609.02780*, 2016.

[47] MG Nomarski. Microinterféromètre différentiel à ondes polarisées. *Journal de Physique et le Radium*, 16:S9–S13, 1955.

[48] Takafumi Ono, Ryo Okamoto, and Shigeki Takeuchi. An entanglement-enhanced microscope. *Nat. Commun.*, 4:2426, Jan 2013.

[49] Chenglong You Kaushik P. Seshadreesan Richard Birrittella Jerome Luine Seyed Mohammad Hashemi Rafsanjani Mohammad Mirhosseini Omar S.Magaña-Loaiza Benjamin E. Koltenbah Claudio G. Parazzoli Barbara A. Capron Robert W. Boyd Christopher C. Gerry Hwang Lee Jonathan P. Dowling Bryan T. Gard, Dong Li. Photon added coherent states: Nondeterministic, noiseless amplification in quantum metrology. 2016.

[50] Peter C. Humphreys, Marco Barbieri, Animesh Datta, and Ian A. Walmsley. Quantum enhanced multiple phase estimation. *Phys. Rev. Lett.*, 111:070403, Aug 2013.

[51] Hwang Lee, Pieter Kok, and Jonathan P. Dowling. A quantum rosetta stone for interferometry. *J. Mod. Opt*, 49(14-15):2325–2338, 2002.

[52] Mario A. Ciampini, Nicolò Spagnolo, Chiara Vitelli, Luca Pezzè, Augusto Smerzi, and Fabio Sciarrino. Quantum-enhanced multiparameter estimation in multiarm interferometers. *Sci. Rep.*, 6:28881, 07 2016.

[53] Vittorio Giovannetti, Seth Lloyd, and Lorenzo Maccone. Advances in quantum metrology. *Nat. Photon.*, 5:222–229, 2011.

[54] Sergio Boixo, Animesh Datta, Steven T. Flammia, Anil Shaji, Emilio Bagan, and Carlton M. Caves. Quantum-limited metrology with product states. *Phys. Rev. A*, 77:012317, Jan 2008.

[55] Bryan T. Gard, Chenglong You, Devendra K. Mishra, Robinjeet Singh, Hwang Lee, Thomas R. Corbitt, and Jonathan P. Dowling. Nearly optimal measurement schemes in a noisy mach-zehnder interferometer with coherent and squeezed vacuum. *EPJ Quantum Technology*, 4(1):4, 2017.

[56] Vincent Daria Joachim Knittel Boris Hage Hans-A. Bachor Michael A. Taylor, Jiri Janousek and Warwick P. Bowen. Biological measurement beyond the quantum limit. *Nat. Photon.*, 7:229–233, 2013.

[57] Marek Piliarik and Vahid Sandoghdar. Direct optical sensing of single unlabelled proteins and super-resolution imaging of their binding sites. *Nat. Comm.*, 5:4495, 2014.

[58] M. R. Andrews, M.-O. Mewes, N. J. van Druten, D. S. Durfee, D. M. Kurn, and W. Ketterle. Direct, nondestructive observation of a bose condensate. *Science*, 273:84–87, 1996.

[59] Michele Celebrano, Philipp Kukura, Alois Renn, and Vahid Sandoghdar. Single-molecule imaging by optical absorption. *Nat. Photon.*, 5:95–98, 2011.

[60] Lu Zhang and Kam Wai Clifford Chan. Quantum multiparameter estimation with generalized balanced multimode noon-like states. *Phys. Rev. A*, 95:032321, 2017.

[61] Pieter Kok, W. J. Munro, Kae Nemoto, T. C. Ralph, Jonathan P. Dowling, and G. J Milburn. Linear optical quantum computing with photonic qubits. *Rev. Mod. Phys*, 79:135–174, 2007.

[62] Hugo Cable and Jonathan P. Dowling. Efficient generation of large number-path entanglement using only linear optics and feed-forward. *Phys. Rev. Lett.*, 99:163604, 2007.

[63] Rafał Demkowicz-Dobrzański, Jan Kołodyński, and Mădălin Guţă. The elusive heisenberg limit in quantum-enhanced metrology. *Nat. Comm.*, 3:1063, 2012.

[64] R. Demkowicz-Dobrzanski, U. Dorner, B. J. Smith, J. S. Lundeen, W. Wasilewski, K. Banaszek, and I. A. Walmsley. Quantum phase estimation with lossy interferometer. *Phys. Rev. A*, 80:013825, 2009.

[65] Giacomo M. D'Ariano and Matteo G. A. Paris. Arbitrary precision in multipath interferometry. *Phys. Rev. A*, 55:2267–2271, 1997.

[66] Scott Aaronson and Alex Arkhipov. The computational complexity of linear optics. In *Proceedings of the Forty-third Annual ACM Symposium on Theory of Computing*, pages 333–342, New York, NY, USA, 2011. ACM.

[67] Bryan T. Gard, Keith R. Motes, Jonathan P. Olson, Peter P. Rohde, and Jonathan P. Dowling. Chapter 8: An introduction to boson-sampling. In *From atomic to mesoscale: The role of quantum coherence in systems of various complexities*, pages 167–192. World Scientific Publishing, 2015.

[68] Justin B. Spring, Benjamin J. Metcalf, Peter C. Humphreys, W. Steven Kolthammer, Xian-Min Jin, Marco Barbieri, Animesh Datta, Nicholas Thomas-Peter, Nathan K. Langford, Dmytro Kundys, James C. Gates, and Bria Smith. Boson sampling on a photonic chip. *Science*, 339:798–801, 2013.

[69] Matthew A Broome, Alessandro Fedrizzi, Saleh Rahimi-Keshari, Justin Dove, Scott Aaronson, Timothy C Ralph, and Andrew G White. Photonic boson sampling in a tunable circuit. *Science*, 339(6121):794–798, 2013.

[70] Andrea Crespi, Roberto Osellame, Roberta Ramponi, Daniel J Brod, Ernesto F Galvao, Nicolo Spagnolo, Chiara Vitelli, Enrico Maiorino, Paolo Mataloni, and Fabio Sciarrino. Integrated multimode interferometers with arbitrary designs for photonic boson sampling. *Nat. Photon.*, 7(7):545–549, 2013.

[71] Nicolò Spagnolo, Chiara Vitelli, Marco Bentivegna, Daniel J. Brod, Andrea Crespi, Fulvio Flamini, Sandro Giacomini, Giorgio Milani, Roberta Ramponi, Paolo Mataloni, Roberto Osellame, and Ernesto F. a Galvão. Experimental validation of photonic boson sampling. *Nat. Photon.*, 8:615–620, 2014.

[72] A P Lund, Michael J Bremner, and T C Ralph. Quantum sampling problems, boson-sampling and quantum supremacy. *NPJ Quantum Information*, 3(1):15, 2017.

[73] Hui Wang, Yu He, Yu-Huai Li, Zu-En Su, Bo Li, He-Liang Huang, Xing Ding, Ming-Cheng Chen, Chang Liu, Jian Qin, Jin-Peng Li, Yu-Ming He, Christian Schneider, Martin Kamp, Cheng-Zhi Peng, and Höfl. High-efficiency multiphoton boson sampling. *Nat. Photon.*, 11:361–365, 2017.

[74] Alex Neville, Chris Sparrow, Raphaël Clifford, Eric Johnston, Patrick M. Birchall, Ashley Montanaro, and Anthony Laing. Classical boson sampling algorithms with superior performance to near-term experiments. *Nat. Phys.*, 10:1153, 2017.

[75] Peter Clifford and Raphaël Clifford. The classical complexity of boson sampling. In *Proceedings of the Twenty-Ninth Annual ACM-SIAM Symposium on Discrete Algorithms*, pages 146–155, Philadelphia, PA, USA, 2018. Society for Industrial and Applied Mathematics.

[76] Igor Aharonovich, Dirk Englund, and Milos Toth. Solid-state single-photon emitters. *Nat. Photon.*, 10:631–641, 2016.

[77] Xing Ding, Yu He, Z.-C. Duan, Niels Gregersen, M.-C. Chen, S. Unsleber, S. Maier, Christian Schneider, Martin Kamp, Sven Höfling, Chao-Yang Lu, and Jian-Wei Pan. On-demand single photons with high extraction efficiency and near-unity indistinguishability from a resonantly driven quantum dot in a micropillar. *Phys. Rev. Lett.*, 116:020401, 2016.

[78] Hui Wang, Z.-C. Duan, Y.-H. Li, Si Chen, J.-P. Li, Y.-M. He, M.-C. Chen, Yu He, X. Ding, Cheng-Zhi Peng, Christian Schneider, Martin Kamp, Sven Höfling, Chao-Yang Lu, and Jian-Wei Pan. Near-transform-limited single photons from an efficient solid-state quantum emitter. *Phys. Rev. Lett.*, 116:213601, 2016.

[79] Xi-Lin Wang, Luo-Kan Chen, W. Li, H.-L. Huang, C. Liu, C. Chen, Y.-H. Luo, Z.-E. Su, D. Wu, Z.-D. Li, H. Lu, Y. Hu, X. Jiang, C.-Z. Peng, L. Li, N.-L. Liu, Yu-Ao Chen, Chao-Yang Lu, and Pan Jian-Wei. Experimental ten-photon entanglement. *Phys. Rev. Lett.*, 117:210502, 2016.

[80] Juan C. Loredo, Nor A. Zakaria, Niccolo Somaschi, Carlos Anton, Lorenzo de Santis, Valerian Giesz, Thomas Grange, Matthew A. Broome, Olivier Gazzano, Guillaume Coppola, Isabelle Sagnes, Aristide Lemaitre, and Alexia Auffev. Scalable performance in solid-state single-photon sources. *Optica*, 3:433–440, 2016.

[81] Jonathan P Olson, Keith R Motes, Patrick M Birchall, Nick M Studer, Margarite LaBorde, Todd Moulder, Peter P Rohde, and Jonathan P Dowling. Linear optical quantum metrology with single photons: Experimental errors, resource counting, and quantum cramér-rao bounds. *Phys. Rev. A*, 96:013810, 2017.

[82] Keith R. Motes, Jonathan P. Olson, Evan J. Rabeaux, Jonathan P. Dowling, S. Jay Olson, and Peter P. Rohde. Linear optical quantum metrology with single photons: Exploiting spontaneously generated entanglement to beat the shot-noise limit. *Phys. Rev. Lett.*, 114:170802, 2015.

[83] Zu-En Su, Yuan Li, Peter P. Rohde, He-Liang Huang, Xi-Lin Wang, Li Li, Nai-Le Liu, Jonathan P. Dowling, Chao-Yang Lu, and Jian-Wei Pan. Multiphoton interference in quantum fourier transform circuits and applications to quantum metrology. *Phys. Rev. Lett.*, 119:080502, 2017.

[84] Joanthan P. Olson. *Complexity Theory and its Applications in Linear Quantum Optics*. PhD thesis, Louisiana State University, 2016.

[85] Marco Bentivegna, Nicolò Spagnolo, Chiara Vitelli, Fulvio Flamini, Niko Viggianiello, Ludovico Latmiral, Paolo Mataloni, Daniel J. Brod, Ernesto F. Galvão, Andrea Crespi, Roberta Ramponi, and Rober Osellame. Experimental scattershot boson sampling. *Sci. Adv.*, 1(3):e1400255, 2015.

[86] Werner Vogel and Dirk-Gunnar Welsch. *Quantum Optics*. John Wiley & Sons, 2006.

[87] Alexander D Poularikas. *Handbook of formulas and tables for signal processing*. CRC Press, 1998.

[88] Keith R Motes, Ryan L Mann, Jonathan P Olson, Nicholas M Studer, E Annelise Bergeron, Alexei Gilchrist, Jonathan P Dowling, Dominic W Berry, and Peter P Rohde. Efficient recycling strategies for preparing large fock states from single-photon sources: Applications to quantum metrology. *Phys. Rev. A*, 94:012344, 2016.

[89] Aaron J. Miller, Adriana E. Lita, Brice Calkins, Igor Vayshenker, Steven M. Gruber, and Sae Woo Nam. Compact cryogenic self-aligning fiber-to-detector coupling with losses below one percent. *Opt. Express*, 19:9102–9110, 2011.

[90] Daiji Fukuda, Go Fujii, Takayuki Numata, Kuniaki Amemiya, Akio Yoshizawa, Hidemi Tsuchida, Hidetoshi Fujino, Hiroyuki Ishii, Taro Itatani, Shuichiro Inoue, and Tatsuya Zama. Titanium-based transition-edge photon number resolving detector with 98% detection efficiency with index-matched small-gap fiber coupling. *Opt. Express*, 19:870–875, 2011.

[91] D Fukuda, G Fujii, T Numata, A Yoshizawa, H Tsuchida, H Fujino, H Ishii, T Itatani, S Inoue, and T Zama. Photon number resolving detection with high speed and high quantum efficiency. *Metrologia*, 46(4):S288–S292, 2009.

[92] L. Dovrat, M. Bakstein, D. Istrati, E. Megidish, A. Halevy, L. Cohen, and H. S. Eisenberg. Direct observation of the degree of correlations using photon-number-resolving detectors. *Phys. Rev. A*, 87:053813, May 2013.

[93] Markus Hijlkema, Bernhard Weber, Holger P. Specht, Simon C. Webster, Axel Kuhn, and Gerhard Rempe. A single-photon server with just one atom. *Nat. Phys.*, 3:253–255, 2007.

[94] R. Lettow, Y. L. A. Rezus, A. Renn, G. Zumofen, E. Ikonen, S. Götzinger, and V. Sandoghdar. Quantum interference of tunably indistinguishable photons from remote organic molecules. *Phys. Rev. Lett.*, 104:123605, 2010.

[95] Christian Kurtsiefer, Sonja Mayer, Patrick Zarda, and Harald Weinfurter. Stable solid-state source of single photons. *Phys. Rev. Lett.*, 85:290–293, 2000.

[96] Andrew J. Shields. Semiconductor quantum light sources. *Nat. Photon.*, 1:215–223, 2007.

[97] A. P. Lund, A. Laing, S. Rahimi-Keshari, T. Rudolph, J. L. O'Brien, and T. C. Ralph. Boson sampling from a gaussian state. *Phys. Rev. Lett.*, 113:100502, Sep 2014.

Appendix A
Reuse and Permissions

The following are the copyright policies of the IOP and APS from:

- Takeoka, M., Seshadreesan, K. P., You, C., Izumi, S., & Dowling, J. P. "Fundamental precision limit of a Mach-Zehnder interferometric sensor when one of the inputs is the vacuum." Phys. Rev. A 96.5 (2017): 052118.

  http://journals.aps.org/copyrightFAQ.html

  As the author of an APS-published article, may I include my article or a portion of my article in my thesis or dissertation?

  Yes, the author has the right to use the article or a portion of the article in a thesis or dissertation without requesting permission from APS, provided the bibliographic citation and the APS copyright credit line are given on the appropriate pages.

- C You, S Adhikari, Y Chi, M L LaBorde, C T Matyas, C Zhang, Z Su, T Byrnes, C Lu, J P Dowling and J P Olson. Multiparameter estimation with single photons–linearly–optically generated quantum entanglement beats the shotnoise limit. Journal of Optics, 19, 124002, 2017.

  https://publishingsupport.iopscience.iop.org/questions/rp-use-of-a-subscription-article-in-your-thesis-or-dissertation-may-i-include-the-final-published-version-of-the-article-in-my-research-thesis-or-dissertation/

  May I include the Final Published Version of the article in my research thesis or dissertation?

  Upon transfer of copyright, IOP and/or the copyright owner grants back to authors a number of rights. These include the right to include the Final Published Version of the article in your research thesis or dissertation. Please include citation details and, for online use, a link to the Version of Record. IOP's permission will be required for commercial use of an article published as part of your thesis. IOP does not allow ProQuest to publish or sell the article as part of your dissertation.

Appendix B
QFI for the MZI with a Vacuum Input

Here we derive Eqs. (3) and (2) in the main text. Consider $|\chi\rangle \otimes |0\rangle$ as an input to the MZ interferometer. For the calculation, it is useful to expand $|\chi\rangle$ in a coherent state basis:

$$|\chi\rangle = \int \mathrm{d}^2\alpha\, f(\alpha)|\alpha\rangle, \tag{B.1}$$

where $|\alpha\rangle$ is a coherent state with complex quadrature amplitude α. Then the average photon number and the variance of the state are given by

$$\begin{aligned}
\bar{n}_\chi &= \langle\chi|\hat{n}|\chi\rangle \\
&= \int \mathrm{d}^2\alpha \int \mathrm{d}^2\beta\, f^*(\alpha) f(\beta) \langle\alpha|\hat{n}|\beta\rangle \\
&= \int \mathrm{d}^2\alpha \int \mathrm{d}^2\beta\, f^*(\alpha) f(\beta) \alpha^*\beta \langle\alpha|\beta\rangle \\
&= \int \mathrm{d}^2\alpha \int \mathrm{d}^2\beta\, f^*(\alpha) f(\beta) \alpha^*\beta \\
&\quad \times \exp\left[-\frac{1}{2}\left(|\alpha|^2 + |\beta|^2 - 2\alpha^*\beta\right)\right],
\end{aligned} \tag{B.2}$$

and

$$\begin{aligned}
V_\chi &= \langle\chi|\hat{n}^2|\chi\rangle - \bar{n}_\chi^2 \\
&= \int \mathrm{d}^2\alpha \int \mathrm{d}^2\beta\, f^*(\alpha) f(\beta) \left\{(\alpha^*\beta)^2 + \alpha^*\beta\right\} \\
&\quad \times \exp\left[-\frac{1}{2}\left(|\alpha|^2 + |\beta|^2 - 2\alpha^*\beta\right)\right] - \bar{n}_\chi^2,
\end{aligned} \tag{B.3}$$

where we use the fact that $\hat{n}^2 = \hat{a}^{\dagger\,2}\hat{a}^2 + \hat{a}^\dagger\hat{a}$.

The state after the beam splitter with transmittance T is given by

$$|\Phi\rangle_{AB} = \int \mathrm{d}^2\alpha\, f(\alpha) \left|\sqrt{T}\alpha\right\rangle_A \left|\sqrt{R}\alpha\right\rangle_B, \tag{B.4}$$

where $R = 1 - T$.

QFI with $\hat{g}_1$ [Eqs. (3)]

The quantum Fisher information (QFI) is calculated from

$$F_Q(|\chi\rangle, \hat{g}_1, T) = 4(\langle\Phi|\hat{g}_1^2|\Phi\rangle - \langle\Phi|\hat{g}_1|\Phi\rangle^2). \tag{B.5}$$

We have

$$\begin{aligned}\langle\Phi|\hat{g}_1^2|\Phi\rangle &= \int \mathrm{d}^2\alpha \int \mathrm{d}^2\beta\, f^*(\alpha)f(\beta) \left\langle \sqrt{T}\alpha\right|_A \left\langle \sqrt{R}\alpha\right|_B \left(\hat{a}^{\dagger\,2}\hat{a}^2 + \hat{a}^\dagger\hat{a}\right) \left|\sqrt{T}\beta\right\rangle_A \left|\sqrt{R}\beta\right\rangle_B \\ &= \int \mathrm{d}^2\alpha \int \mathrm{d}^2\beta\, f^*(\alpha)f(\beta) \left\{(T\alpha^*\beta)^2 + T\alpha^*\beta\right\} \left\langle \sqrt{T}\alpha\right| \left.\sqrt{T}\beta\right\rangle \left\langle \sqrt{R}\alpha\right| \left.\sqrt{R}\beta\right\rangle \\ &= T^2\langle\chi|\hat{n}^2|\chi\rangle + T(1-T)\langle\chi|\hat{n}|\chi\rangle, \end{aligned} \tag{B.6}$$

and

$$\begin{aligned}\langle\Phi|\hat{g}_1|\Phi\rangle^2 &= \left(\int \mathrm{d}^2\alpha \int \mathrm{d}^2\beta\, f^*(\alpha)f(\beta) \left\langle \sqrt{T}\alpha\right|_A \left\langle \sqrt{R}\alpha\right|_B \left(\hat{a}^\dagger\hat{a}\right) \left|\sqrt{T}\beta\right\rangle_A \left|\sqrt{R}\beta\right\rangle_B\right)^2 \\ &= T^2\langle\chi|\hat{n}|\chi\rangle^2. \end{aligned} \tag{B.7}$$

In total, we have

$$F_Q(|\chi\rangle, \hat{g}_1, T) = 4(\langle\Phi|\hat{g}_1^2|\Phi\rangle - \langle\Phi|\hat{g}_1|\Phi\rangle^2) = 4\left\{T^2V_\chi + T(1-T)\bar{n}_\chi\right\}. \tag{B.8}$$

For $T = 1/2$, it is $V_\chi + \bar{n}_\chi$ and thus we get Eq. (3).

QFIM for $\hat{g}_d$ and $\hat{g}_s$ [Eqs. (2)]

For pure states, the elements of the QFIM are given by

$$F_{ij} = 4\left(\langle\hat{g}_i\hat{g}_j\rangle - \langle\hat{g}_i\rangle\langle\hat{g}_j\rangle\right), \tag{B.9}$$

where i, j takes s and d.

Recall that $\hat{g}_d = (\hat{a}^\dagger\hat{a} - \hat{b}^\dagger\hat{b})/2$ and $\hat{g}_s = (\hat{a}^\dagger\hat{a} + \hat{b}^\dagger\hat{b})/2$. Then we have

$$\begin{aligned}4\langle\Phi|\hat{g}_d^2|\Phi\rangle &= \int \mathrm{d}^2\alpha \int \mathrm{d}^2\beta\, f^*(\alpha)f(\beta) \\ &\quad \times \left\langle \sqrt{T}\alpha\right|_A \left\langle \sqrt{R}\alpha\right|_B \left(\hat{a}^{\dagger\,2}\hat{a}^2 + \hat{a}^\dagger\hat{a} + \hat{b}^{\dagger\,2}\hat{b}^2 + \hat{b}^\dagger\hat{b} - 2\hat{a}^\dagger\hat{a}\hat{b}^\dagger\hat{b}\right) \left|\sqrt{T}\beta\right\rangle_A \left|\sqrt{R}\beta\right\rangle_B \\ &= \int \mathrm{d}^2\alpha \int \mathrm{d}^2\beta\, f^*(\alpha)f(\beta) \\ &\quad \times \left\{(T\alpha^*\beta)^2 + T\alpha^*\beta + (R\alpha^*\beta)^2 + R\alpha^*\beta - 2RT(\alpha^*\beta)^2\right\} \left\langle \sqrt{T}\alpha\right| \left.\sqrt{T}\beta\right\rangle \left\langle \sqrt{R}\alpha\right| \left.\sqrt{R}\beta\right\rangle \\ &= \int \mathrm{d}^2\alpha \int \mathrm{d}^2\beta\, f^*(\alpha)f(\beta) \left\{\alpha^*\beta + (T-R)^2(\alpha^*\beta)^2\right\} \exp\left[-\frac{1}{2}\left(|\alpha|^2 + |\beta|^2 - 2\alpha^*\beta\right)\right] \\ &= \langle\chi|\hat{n}|\chi\rangle + (1-2T)^2\left(\langle\chi|\hat{n}^2|\chi\rangle - \langle\chi|\hat{n}|\chi\rangle\right). \end{aligned} \tag{B.10}$$

Similarly, we have

$$4\langle\Phi|\hat{g}_s^2|\Phi\rangle = \langle\chi|\hat{n}^2|\chi\rangle, \tag{B.11}$$

$$4\langle\Phi|\hat{g}_d\hat{g}_s|\Phi\rangle = 4\langle\Phi|\hat{g}_s\hat{g}_d|\Phi\rangle = -(1-2T)\langle\chi|\hat{n}^2|\chi\rangle. \tag{B.12}$$

Also

$$\begin{aligned}
2\langle\Phi|\hat{g}_d|\Phi\rangle &= \int \mathrm{d}^2\alpha \int \mathrm{d}^2\beta\, f^*(\alpha)f(\beta) \left\langle \sqrt{T}\alpha\right|_A \left\langle \sqrt{R}\alpha\right|_B \left(\hat{a}^\dagger\hat{a} - \hat{b}^\dagger\hat{b}\right) \left|\sqrt{T}\beta\right\rangle_A \left|\sqrt{R}\beta\right\rangle_B \\
&= \int \mathrm{d}^2\alpha \int \mathrm{d}^2\beta\, f^*(\alpha)f(\beta)\left(T\alpha^*\beta - R\alpha^*\beta\right) \left\langle \sqrt{T}\alpha\right| \left.\sqrt{T}\beta\right\rangle \left\langle \sqrt{R}\alpha\right| \left.\sqrt{R}\beta\right\rangle \\
&= (1-2T)\int \mathrm{d}^2\alpha \int \mathrm{d}^2\beta\, f^*(\alpha)f(\beta)\alpha^*\beta \exp\left[-\frac{1}{2}\left(|\alpha|^2 + |\beta|^2 - 2\alpha^*\beta\right)\right] \\
&= (1-2T)\langle\chi|\hat{n}|\chi\rangle, \qquad \text{(B.13)}
\end{aligned}$$

and similarly,

$$2\langle\Phi|\hat{g}_s|\Phi\rangle = \langle\chi|\hat{n}|\chi\rangle. \qquad \text{(B.14)}$$

By using the above results, we have

$$\begin{aligned}
F_{dd} &= F_Q(|\chi\rangle, \hat{g}_d, T) \\
&= \langle\chi|\hat{n}|\chi\rangle + (1-2T)^2\left(\langle\chi|\hat{n}^2|\chi\rangle - \langle\chi|\hat{n}|\chi\rangle\right) \\
&\quad -(1-2T)^2\langle\chi|\hat{n}|\chi\rangle^2 \\
&= \left\{1-(1-2T)^2\right\}\bar{n}_\chi + (1-2T)^2 V_\chi, \qquad \text{(B.15)}
\end{aligned}$$

$$\begin{aligned}
F_{ss} &= \langle\chi|\hat{n}^2|\chi\rangle - \langle\chi|\hat{n}|\chi\rangle^2 \\
&= V_\chi, \qquad \text{(B.16)} \\
F_{ds} &= F_{sd} = -(1-2T)\langle\chi|\hat{n}^2|\chi\rangle - (1-2T)\langle\chi|\hat{n}|\chi\rangle^2 \\
&= -(1-2T)V_\chi. \qquad \text{(B.17)}
\end{aligned}$$

Appendix C
Convexity of QFI Matrix

Here we prove the convexity of the quantum Fisher information matrix (QFIM):

$$\mathcal{F}_Q(\hat{\rho}_\varphi) \leq p\mathcal{F}_Q(\hat{\sigma}_\varphi) + (1-p)\mathcal{F}_Q(\hat{\tau}_\varphi), \tag{C.1}$$

for $\hat{\rho}_\varphi = p\hat{\sigma}_\varphi + (1-p)\hat{\tau}_\varphi$. Here $\hat{\rho}_\varphi$, $\hat{\sigma}_\varphi$, and $\hat{\tau}_\varphi$ are (maybe mixed) quantum states where $\varphi = \{\varphi_1, \ldots, \varphi_M\}$ is a set of M unknown parameters.

To begin with, we briefly review the definition and the structure of the QFIM that we will use in the proof. Detailed review on the QFI and QFIM can be found for example in Ref. [35, 15, 37]. The QFIM for $\hat{\rho}_\varphi$ is given by an $M \times M$ matrix $\mathcal{F}_Q(\hat{\rho}_\varphi) = [F_{ij}(\hat{\rho}_\varphi)]_{ij}$ $(i, j = 1, \ldots, M)$ where each entry is defined as

$$F_{ij}(\hat{\rho}_\varphi) = \frac{1}{2}\mathrm{Tr}\left[\hat{\rho}_\varphi \hat{L}_i \hat{L}_j + \hat{\rho}_\varphi \hat{L}_j \hat{L}_i\right], \tag{C.2}$$

and $\hat{L}_i$, called the symmetrized logarithmic derivative, is a Hermitian operator satisfying

$$\frac{\partial}{\partial \varphi_i}\hat{\rho}_\varphi = \frac{1}{2}\left(\hat{L}_i\hat{\rho}_\varphi + \hat{\rho}_\varphi\hat{L}_i\right). \tag{C.3}$$

Let $\hat{\rho}_\varphi = \sum_k \lambda_k |\lambda_k\rangle\langle\lambda_k|$ be the spectral decomposition of $\hat{\rho}_\varphi$. Then we can explicitly describe $\hat{L}_i$ as

$$\hat{L}_i = 2\sum_{k,l} \frac{\langle\lambda_k|\hat{\rho}_\varphi^{(i)}|\lambda_l\rangle}{\lambda_k + \lambda_l}|\lambda_k\rangle\langle\lambda_l|, \tag{C.4}$$

where $\hat{\rho}_\varphi^{(i)} = \partial\hat{\rho}_\varphi/\partial\varphi_i$. Combining it with Eq. (C.2), the QFIM is expressed as

$$F_{ij}(\hat{\rho}_\varphi) = 2\sum_{k,l} \frac{\langle\lambda_k|\hat{\rho}_\varphi^{(i)}|\lambda_l\rangle\langle\lambda_l|\hat{\rho}_\varphi^{(j)}|\lambda_k\rangle}{\lambda_k + \lambda_l}. \tag{C.5}$$

We also use an important property of the QFIM: monotonicity under completely positive trace preserving (CPTP) map $\mathcal{L}$ [36, 37],

$$\mathcal{F}_Q(\hat{\rho}_\varphi) \geq \mathcal{F}_Q(\mathcal{L}(\hat{\rho}_\varphi)). \tag{C.6}$$

The proof of the convexity of the QFIM is basically given by extending the proof for the QFI (i.e. single-parameter case) in Ref. [38]. Consider the bipartite state $\tilde{\rho}_\varphi^{AB} = p|e_0\rangle\langle e_0|^A \otimes \hat{\sigma}_\varphi^B + (1-p)|e_1\rangle\langle e_1|^A \otimes \hat{\tau}_\varphi^B$, where $|e_k\rangle$ is an orthonormal basis in A. Note that $\mathrm{Tr}_A[\tilde{\rho}_\varphi^{AB}] = \hat{\rho}_\varphi^B$. Then we have

$$\mathcal{F}_Q(\tilde{\rho}_\varphi^{AB}) = p\mathcal{F}_Q(\hat{\sigma}_\varphi^B) + (1-p)\mathcal{F}_Q(\hat{\tau}_\varphi^B). \tag{C.7}$$

This is justified by the following observation. Since $|e_k\rangle$ is independent of the unknown parameters φ_i, $\tilde{\rho}_\varphi^{(i)} = p|e_0\rangle\langle e_0| \otimes \hat{\sigma}_\varphi^{(i)} + (1-p)|e_1\rangle\langle e_1| \otimes \hat{\tau}_\varphi^{(i)}$, for any i. Also the spectral de-

composition of $\tilde{\rho}_\varphi$ is described as $p|e_0\rangle\langle e_0| \otimes \sum_i \lambda_i^\sigma |\lambda_i^\sigma\rangle\langle\lambda_i^\sigma| + (1-p)|e_1\rangle\langle e_1| \otimes \sum_i \lambda_i^\tau |\lambda_i^\tau\rangle\langle\lambda_i^\tau|$, where $\sum_i \lambda_i^\sigma |\lambda_i^\sigma\rangle\langle\lambda_i^\sigma|$ and $\sum_i \lambda_i^\tau |\lambda_i^\tau\rangle\langle\lambda_i^\tau|$ are the spectral decompositions of $\hat{\sigma}_\varphi$ and $\hat{\tau}_\varphi$, respectively. Plugging them into the expression of QFI in Eq. (C.5), we get

$$F_{ij}(\tilde{\rho}_\varphi^{AB}) = pF_{ij}(\hat{\sigma}_\varphi^B) + (1-p)F_{ij}(\hat{\tau}_\varphi^B). \tag{C.8}$$

Since this holds for all i and j, we get Eq. (C.7).

By using Eq. (C.7), the monotonicity (C.6), and the fact that partial trace is a CPTP map, we have

$$\begin{aligned} \mathcal{F}_Q(\hat{\rho}_\varphi^B) &\leq \mathcal{F}_Q(\hat{\rho}_\varphi^{AB}) \\ &= p\mathcal{F}_Q(\hat{\sigma}_\varphi^B) + (1-p)\mathcal{F}_Q(\hat{\tau}_\varphi^B), \end{aligned} \tag{C.9}$$

which completes the proof of the convexity of the QFIM.

Appendix D
QFI of MZI for $\hat{g}_1$ with Phase Randomizing

Here we give a complete calculation of the QFI for the generator $\hat{g}_1 = \hat{a}^\dagger \hat{a}$ with phase randomizing. The two input states are a vacuum and an arbitrary quantum state with the density matrix of

$$\hat{\rho}_{\rm in} = \sum_{n,m=0}^{\infty} c_{nm} |n\rangle\langle m|, \tag{D.1}$$

where $|n\rangle$ is the n-photon number state. Then the phase-averaged input is given by

$$\begin{aligned} \Psi_{\rm avg} &= \int \frac{d\theta}{2\pi} \hat{V}_\theta^A \hat{V}_\theta^B \left(\hat{\rho}_{\rm in}^A \otimes |0\rangle\langle 0|^B \right) \hat{V}_\theta^{A\,\dagger} \hat{V}_\theta^{B\,\dagger} \\ &= \sum_{n,m=0}^{\infty} \int \frac{d\theta}{2\pi} e^{i\theta(n-m)} c_{nm} |n\rangle\langle m|^A \otimes |0\rangle\langle 0|^B \\ &= \sum_{n=0}^{\infty} p_n |n\rangle\langle n|^A \otimes |0\rangle\langle 0|^B, \end{aligned} \tag{D.2}$$

where $\hat{V}_\theta^A = e^{i\theta \hat{a}^\dagger \hat{a}}$, $\hat{V}_\theta^B = e^{i\theta \hat{b}^\dagger \hat{b}}$, and $p_n = c_{nn}$ is a real positive number satisfying $\sum_n p_n = 1$. The state after the first beamsplitter of the MZI and the phase shifting is given by

$$\begin{aligned} \Psi_{\rm avg}^\phi &= \hat{U}_\phi^{(1)\,AB} \hat{B}_T^{AB} \Psi_{\rm avg} \hat{B}_T^{\dagger AB} \hat{U}_\phi^{(1)\dagger\,AB} \\ &= \sum_{n=0}^{\infty} p_n |\psi_n(\phi)\rangle\langle\psi_n(\phi)|_{AB}, \end{aligned} \tag{D.3}$$

where

$$\begin{aligned} |\psi_n(\phi)\rangle_{AB} &= \sum_{j=0}^{n} e^{-ij\phi} \binom{n}{j}^{1/2} \\ &\quad \times T^{j/2} (1-T)^{(n-j)/2} |j\rangle_A \otimes |n-j\rangle_B. \end{aligned} \tag{D.4}$$

By using the convexity of the QFI and noticing that $|\psi_n(\phi)\rangle$ and $|\psi_{n'}(\phi)\rangle$ are orthogonal for $n \neq n'$, we have

$$F_Q^{(1)} \left(\Psi_{\rm avg}^\phi \right) = \sum_{n=0}^{\infty} p_n F_Q^{(1)} \left(|\psi_n(\phi)\rangle \right). \tag{D.5}$$

Thus our remaining task is to calculate $F_Q^{(1)}\left(|\psi_n(\phi)\rangle\right)$ explicitly. For $|\psi_n(\phi)\rangle$, we find

$$\langle \hat{a}^\dagger \hat{a} \rangle = \sum_{j=0}^{n} j \binom{n}{j} T^j \left(1-T\right)^{n-j} = nT, \tag{D.6}$$

$$\langle \hat{b}^\dagger \hat{b} \rangle = n\left(1-T\right), \tag{D.7}$$

$$\begin{aligned} \langle \hat{a}^{\dagger 2} \hat{a}^2 \rangle &= \sum_{j=0}^{n} j\left(j-1\right) \binom{n}{j} T^j \left(1-T\right)^{n-j} \\ &= n(n-1)T^2, \end{aligned} \tag{D.8}$$

and the QFI evaluated as $4\left(\langle \hat{g}_1^2 \rangle - \langle \hat{g}_1 \rangle^2\right)$ is found to be

$$\begin{aligned} F_Q^{(1)}(|\psi_n(\phi)\rangle) &= 4\left(\langle \hat{a}^{\dagger 2}\hat{a}^2 \rangle + \langle \hat{a}^\dagger \hat{a} \rangle - \langle \hat{a}^\dagger \hat{a} \rangle^2\right) \\ &= 4\left\{n(n-1)T^2 + nT - n^2T^2\right\} \\ &= 4nT\left(1-T\right). \end{aligned} \tag{D.9}$$

Then averaging over n, we get

$$F_Q^{(1)}\left(\Psi_{\text{avg}}^{\phi}\right) = 4\bar{n}T(1-T), \tag{D.10}$$

The maximum is attained at $T = 1/2$ and is equal to $\bar{n}$.

Appendix E
Calculation of QFI for SU(1,1) Interferometers

Phase in Upper Arm

Our input state is $|\Psi_{in}\rangle = |0\rangle \otimes |\chi\rangle$. The Quantum Fisher information (QFI) is given by:

$$F = 4\left(\langle\Psi_{in}|(a_1^\dagger a_1)^2|\Psi_{in}\rangle - \langle\Psi_{in}|a_1^\dagger a_1|\Psi_{in}\rangle^2\right) \tag{E.1}$$

For simplicity, let us break down the calculation step by step. For the calculation of second term, the $a_1^\dagger a_1$ term can be written as:

$$a_1^\dagger a_1 = u^2 a_0^\dagger a_0 + |\nu|^2 b_0 b_0^\dagger + u\nu a_0^\dagger b_0^\dagger + u\nu^* a_0 b_0. \tag{E.2}$$

Only one term gives a non-zero element, giving

$$\begin{aligned}\langle\Psi_{in}|a_1^\dagger a_1|\Psi_{in}\rangle &= \langle 0|\otimes\langle\chi|(b_0 b_0^\dagger \sinh^2 r)|0\rangle\otimes|\chi\rangle \\ &= \sinh^2 r\langle\chi|b_0 b_0^\dagger|\chi\rangle \\ &= \sinh^2 r(\langle b_0^\dagger b_0\rangle + 1).\end{aligned} \tag{E.3}$$

The $(a_1^\dagger a_1)^2$ can be written as:

$$\begin{aligned}(a_1^\dagger a_1)^2 = {} & u^4 a_0^\dagger a_0 a_0^\dagger a_0 + u^3\nu a_0^\dagger a_0 a_0^\dagger b_0^\dagger + u^3\nu^* a_0^\dagger a_0 a_0 b_0 + u^2|\nu|^2 a_0^\dagger a_0 b_0 b_0^\dagger \\ & + u^3\nu a_0^\dagger a_0^\dagger a_0 b_0^\dagger + u^2\nu^2 a_0^\dagger a_0^\dagger b_0^\dagger b_0^\dagger + u^2|\nu|^2 a_0^\dagger a_0 b_0^\dagger b_0 + u|\nu|^2\nu a_0^\dagger b_0^\dagger b_0 b_0^\dagger \\ & + u^3\nu^* a_0 a_0^\dagger a_0 b_0 + u^2|\nu|^2 a_0 a_0^\dagger b_0 b_0^\dagger + u^2\nu^{*2} a_0 a_0 b_0 b_0 + u|\nu|^2\nu^* a_0 b_0 b_0 b_0^\dagger \\ & + u^2|\nu|^2 a_0^\dagger a_0 b_0 b_0^\dagger + u|\nu|^2\nu a_0^\dagger b_0 b_0^\dagger b_0^\dagger + u|\nu|^2\nu^* a_0 b_0 b_0^\dagger b_0 + |\nu|^4 b_0 b_0^\dagger b_0 b_0^\dagger.\end{aligned} \tag{E.4}$$

The above term can be multiplied as before. Only two terms survives to give:

$$\begin{aligned}&\langle 0|\otimes\langle\chi|(a_0 a_0^\dagger b_0 b_0^\dagger \sinh^2 r\cosh^2 r)|0\rangle\otimes|\chi\rangle \\ &= \sinh^2 r\cosh^2 r\langle 0|a_0 a_0^\dagger 0\rangle\langle\chi|b_0 b_0^\dagger|\chi\rangle \\ &= \sinh^2 r\cosh^2 r(\langle b_0^\dagger b_0\rangle + 1).\end{aligned} \tag{E.5}$$

And,

$$\begin{aligned}&\langle 0|\otimes\langle\chi|(b_0 b_0^\dagger b_0 b_0^\dagger \sinh^4 r)|0\rangle\otimes|\chi\rangle \\ &= \sinh^4 r\langle\chi|b_0 b_0^\dagger b_0 b_0^\dagger|\chi\rangle \\ &= \sinh^4 r\langle\chi|(b_0^\dagger b_0 + 1)(b_0^\dagger b_0 + 1)|\chi\rangle \\ &= \sinh^4 r\langle\chi|(b_0^\dagger b_0)^2 + 2b_0^\dagger b_0 + 1|\chi\rangle \\ &= \sinh^4 r(\langle(b_0^\dagger b_0)^2\rangle + 2\langle b_0^\dagger b_0\rangle + 1).\end{aligned} \tag{E.6}$$

Then, the first term of the QFI is given by:

$$\langle\Psi_{in}|(a_1^\dagger a_1)^2|\Psi_{in}\rangle = \sinh^4 r(\langle(b_0^\dagger b_0)^2\rangle + 2\langle b_0^\dagger b_0\rangle + 1) + \sinh^2 r\cosh^2 r(\langle b_0^\dagger b_0\rangle + 1) \tag{E.7}$$

Hence, the Quantum Fisher information (QFI) is:

$$\begin{aligned} F = 4\sinh^2 r\cosh^2 r(\langle b_0^\dagger b_0\rangle + 1) + 4\sinh^4 r(\langle(b_0^\dagger b_0)^2\rangle \\ + 2\langle b_0^\dagger b_0\rangle + 1) - 4(\sinh^2 r(\langle b_0^\dagger b_0\rangle + 1))^2 \end{aligned}$$

Phase in Lower Arm

Similar to the last calculation, let's break down the calculation step by step. . The $b_1^\dagger b_1$ can be written as:

$$b_1^\dagger b_1 = |\nu|^2 a_0 a_0^\dagger + u^2 b_0^\dagger b_0 + u\nu a_0^\dagger b_0^\dagger + u\nu^* a_0 b_0. \tag{E.8}$$

Only two of the term gives a non-zero element.

$$\begin{aligned} &\langle 0|\otimes\langle\chi|b_0^\dagger b_0\cosh^2 r|0\rangle\otimes|\chi\rangle \\ &= \cosh^2 r\langle\chi|b_0^\dagger b_0|\chi\rangle \\ &= \cosh^2 r\langle b_0^\dagger b_0\rangle \end{aligned} \tag{E.9}$$

And,

$$\langle 0|\otimes\langle\chi|a_0 a_0^\dagger\sinh^2 r|0\rangle\otimes|\chi\rangle = \sinh^2 r. \tag{E.10}$$

Hence,

$$\langle\Psi_{in}|b_1^\dagger b_1|\Psi_{in}\rangle = \cosh^2 r\langle b_0^\dagger b_0\rangle + \sinh^2 r \tag{E.11}$$

Similarly, $(b_1^\dagger b_1)^2$ can be written as:

$$\begin{aligned} (b_1^\dagger b_1)^2 = &|\nu|^4 a_0 a_0^\dagger a_0 a_0^\dagger + u^2|\nu|^2 a_0 a_0^\dagger b_0^\dagger b_0 + u|\nu|^2\nu a_0 a_0^\dagger a_0^\dagger b_0^\dagger + u|\nu|^2\nu^* a_0 a_0^\dagger a_0 b_0 \\ &+ u^2|\nu|^2 a_0 a_0^\dagger b_0^\dagger b_0 + u^4 b_0^\dagger b_0 b_0^\dagger b_0 + u^3\nu a_0^\dagger b_0^\dagger b_0 b_0^\dagger + u^3\nu^* a_0 b_0^\dagger b_0 b_0 \\ &+ u|\nu|^2\nu a_0^\dagger a_0 a_0^\dagger b_0^\dagger + u^3\nu a_0^\dagger b_0^\dagger b_0^\dagger b_0 + u^2\nu^2 a_0^\dagger a_0^\dagger b_0^\dagger b_0^\dagger + u^2|\nu|^2 a_0^\dagger a_0 b_0^\dagger b_0 \\ &+ u|\nu|^2\nu^* a_0 a_0 a_0^\dagger b_0 + u^3\nu^* a_0 b_0 b_0^\dagger b_0 + u^2|\nu|^2 a_0 a_0^\dagger b_0 b_0^\dagger + u^2\nu^{*2} a_0 a_0 b_0 b_0. \end{aligned} \tag{E.12}$$

The above term can be multiplied as before. Only four terms survives giving:

$$\begin{aligned} &\langle 0|\otimes\langle\chi|\left(a_0 {a_0}^\dagger\right)^2|0\rangle\otimes|\chi\rangle = \sinh^4 r, \\ &\langle 0|\otimes\langle\chi|\, a_0 {a_0}^\dagger {b_0}^\dagger b_0\,|0\rangle\otimes|\chi\rangle = \langle b_0^\dagger b_0\rangle\sinh^2 r\cosh^2 r, \\ &\langle 0|\otimes\langle\chi|\left({b_0}^\dagger b_0\right)^2|0\rangle\otimes|\chi\rangle = \langle(b_0^\dagger b_0)^2\rangle\cosh^4 r, \\ &\langle 0|\otimes\langle\chi|\, a_0 {a_0}^\dagger b_0 {b_0}^\dagger\,|0\rangle\otimes|\chi\rangle = (\langle b_0^\dagger b_0\rangle + 1)\sinh^2 r\cosh^2 r. \end{aligned} \tag{E.13}$$

And,

$$\langle\Psi_{in}|(b_1^\dagger b_1)^2|\Psi_{in}\rangle = \sinh^4 r + 3\sinh^2 r\cosh^2 r\langle {b_0}^\dagger b_0\rangle + \cosh^4 r\langle(b_0^\dagger b_0)^2\rangle + \sinh^2 r\cosh^2 r. \quad \text{(E.14)}$$

Hence, the Fisher information is given by:

$$\begin{aligned} F &= 4\left(\langle\Psi_{in}|(b_1^\dagger b_1)^2|\Psi_{in}\rangle - \langle\Psi_{in}|b_1^\dagger b_1|\Psi_{in}\rangle^2\right) \\ F &= 4(\sinh^4 r + 3\langle b_0^\dagger b_0\rangle\sinh^2\cosh^2 r + \langle(b_0^\dagger b_0)^2\rangle\cosh^4 r + \sinh^2\cosh^2 r) \\ &\quad - 4(\sinh^2 r + \langle b_0^\dagger b_0\rangle\cosh^2 r)^2 \end{aligned} \quad \text{(E.15)}$$

Phase in Both Arms

Similar to the previous calculation. The $a_1^\dagger a_1 + b_1^\dagger b_1$ and $(a_1^\dagger a_1 + b_1^\dagger b_1)^2$ terms can be written as:

$$\begin{aligned} a_1^\dagger a_1 + b_1^\dagger b_1 = (a_0 a_0^\dagger + b_0 b_0^\dagger)\cosh 2r + 2\sinh^2 r \\ + 2a_0^\dagger b_0^\dagger e^{-i\theta}\cosh r\sinh r + 2a_0 b_0 e^{i\theta}\sinh r\cosh r. \end{aligned} \quad \text{(E.16)}$$

Only two of them gives a non-zero term.

$$\langle 0|\otimes\langle\chi|b_0 b_0^\dagger\cosh 2r|0\rangle\otimes|\chi\rangle = \cosh 2r\langle b_0^\dagger b_0\rangle + \cosh 2r, \quad \text{(E.17)}$$

$$\langle 0|\otimes\langle\chi|2\sinh r|0\rangle\otimes|\chi\rangle = 2\sinh r. \quad \text{(E.18)}$$

Hence,

$$\langle\Psi_{in}|a_1^\dagger a_1 + b_1^\dagger b_1|\Psi_{in}\rangle = \cosh 2r\langle b_0^\dagger b_0\rangle + 2\sinh r \quad \text{(E.19)}$$

Similarly,

$$\begin{aligned} \langle\Psi_{in}|(a_1^\dagger a_1 + b_1^\dagger b_1)^2|\Psi_{in}\rangle = 4\sinh^4 r + 4\sinh^2 r\cosh 2r\langle {b_0}^\dagger b_0\rangle + \cosh^2 2r\langle(b_0^\dagger b_0)^2\rangle \\ + 4\sinh^2 r\cosh^2 r\langle {b_0}^\dagger b_0\rangle + 4\sinh^2 r\cosh^2 r. \end{aligned} \quad \text{(E.20)}$$

Hence, the QFI is:

$$\begin{aligned} F &= 4\left(\langle\Psi_{in}|(a_1^\dagger a_1 + b_1^\dagger b_1)^2|\Psi_{in}\rangle - \langle\Psi_{in}|a_1^\dagger a_1 + b_1^\dagger b_1|\Psi_{in}\rangle^2\right) \\ &= \cosh^2(2r)\left[\left\langle\left(b_0^\dagger b_0\right)^2\right\rangle - \left\langle b_0^\dagger b_0\right\rangle^2\right] + \sinh^2(2r)\left[1 + \left\langle b_0^\dagger b_0\right\rangle\right] \end{aligned} \quad \text{(E.21)}$$

Appendix F
Calculation of QFI Matrix

Here we calculate the entries of the QFI matrix $\mathcal{F}_{\vec{\varphi}}$. In general, they are specified by,

$$[\mathcal{F}_{\vec{\varphi}}]_{l,n} = 4\left\langle \hat{b}_l^\dagger \hat{b}_l \hat{b}_n^\dagger \hat{b}_n \right\rangle - 4\left\langle \hat{b}_l^\dagger \hat{b}_l \right\rangle \left\langle \hat{b}_n^\dagger \hat{b}_n \right\rangle. \tag{F.1}$$

Computing the latter term first,

$$\begin{aligned} \langle\psi|\hat{b}_j^\dagger \hat{b}_j|\psi\rangle &= \textstyle\sum_{q,l=1}^m V_{j,q}\bar{V}_{j,l}\langle k|^{\otimes m}\hat{a}_q^\dagger \hat{a}_l|k\rangle^{\otimes m} \\ &= \textstyle\sum_{q=1}^m |V_{j,q}|^2\langle k|^{\otimes m}\hat{a}_q^\dagger \hat{a}_q|k\rangle^{\otimes m} \\ &= \textstyle\sum_{q=1}^m \frac{1}{m}\cdot k \\ &= k. \end{aligned} \tag{F.2}$$

Hence,

$$4\left\langle \hat{b}_l^\dagger \hat{b}_l \right\rangle \left\langle \hat{b}_n^\dagger \hat{b}_n \right\rangle = 4k^2. \tag{F.3}$$

Meanwhile,

$$\langle\psi|\hat{b}_l^\dagger \qquad \hat{b}_l \hat{b}_n^\dagger \hat{b}_n|\psi\rangle \tag{F.4}$$

$$= \textstyle\sum_{i,j,q,p=1}^m V_{l,i}\bar{V}_{l,j}V_{n,q}\bar{V}_{n,p}\langle k|^{\otimes m}\hat{a}_i^\dagger \hat{a}_j \hat{a}_q^\dagger \hat{a}_p|k\rangle^{\otimes m} \tag{F.5}$$

$$\begin{aligned} &= \textstyle\sum_{q,p,q\neq p}^m V_{l,p}\bar{V}_{l,q}V_{n,q}\bar{V}_{n,p}\langle k|^{\otimes m}\hat{a}_p^\dagger \hat{a}_q \hat{a}_q^\dagger \hat{a}_p|k\rangle^{\otimes m} \\ &\quad + \textstyle\sum_{q,p}^m |V_{l,p}|^2|V_{n,q}|^2\langle k|^{\otimes m}\hat{a}_p^\dagger \hat{a}_p \hat{a}_q^\dagger \hat{a}_q|k\rangle^{\otimes m}. \end{aligned} \tag{F.6}$$

The second term here is essentially just the square of Eq. (F.2), and equal to k^2, hence,

$$= k^2 + \textstyle\sum_{q,p,q\neq p}^m (V_{l,p}\bar{V}_{l,q}V_{n,q}\bar{V}_{n,p})k(k+1) \tag{F.7}$$

Then we have to evaluate,

$$\sum_{q,p=1,q\neq p}^{m} (V_{l,p}\bar{V}_{l,q}V_{n,q}\bar{V}_{n,p}). \tag{F.8}$$

Rewriting $\omega = e^{2\pi i/m}$ as the first mth root of unity,

$$= \tfrac{1}{m^2} \sum_{q,p=1,q\neq p}^{m} \omega^{(l-1)(p-1)}\omega^{-(l-1)(q-1)}\omega^{(n-1)(q-1)}\omega^{-(n-1)(p-1)} \tag{F.9}$$

$$= \tfrac{1}{m^2} \textstyle\sum_{q,p=1,q\neq p}^m \left[\omega^{(p-q)}\right]^{(l-1)}\left[\omega^{(q-p)}\right]^{(n-1)} \tag{F.10}$$

$$= \tfrac{1}{m^2} \textstyle\sum_{q,p=1,q\neq p}^m \left[\omega^{(p-q)}\right]^{(l-1)}\left[\omega^{-(p-q)}\right]^{(n-1)} \tag{F.11}$$

$$= \tfrac{1}{m^2} \textstyle\sum_{q,p=1,q\neq p}^m \left[\omega^{(p-q)}\right]^{l-n} \tag{F.12}$$

If $l - n = 0$, i.e. for the diagonal entries of $\mathcal{F}_{\boldsymbol{\varphi}}^{\text{quant}}$, the summand is 1 and hence the sum evaluates to $m^2 - m$. For the off-diagonal terms, let $l - n = k$, so

$$= \frac{1}{m^2} \sum_{q,p=1,q\neq p}^{m} \left[\omega^{(p-q)}\right]^k \tag{F.13}$$

$$= \frac{1}{m^2} \sum_{q,p=1,q\neq p}^{m} \left[\omega^k\right]^{(p-q)} \tag{F.14}$$

Let $p - q = r$, and note that $r \neq 0$. There are m-many $\{p, q\}$ pairs whose difference is r (or congruent to $r(\text{mod } m)$, since ω is a mth root of unity). Thus the sum reduces to,

$$= \frac{1}{m^2}[m \sum_{r=1}^{m-1} \left[\omega^k\right]^r] \tag{F.15}$$

$$= \frac{1}{m^2}[m[-1]] \tag{F.16}$$

$$= -\frac{1}{m}, \tag{F.17}$$

where we have used the fact that the sum over all powers of any kth root of unity is equal to one. Thus, the terms of the QFI matrix simplify to,

$$[\mathcal{F}_{\vec{\boldsymbol{\varphi}}}]_{l,n} = \begin{cases} 4k(k+1) \cdot \frac{m-1}{m} & l = m \\ 4k(k+1) \cdot -\frac{1}{m} & l \neq m \end{cases} . \tag{F.18}$$

Appendix G
Sequential QUMI

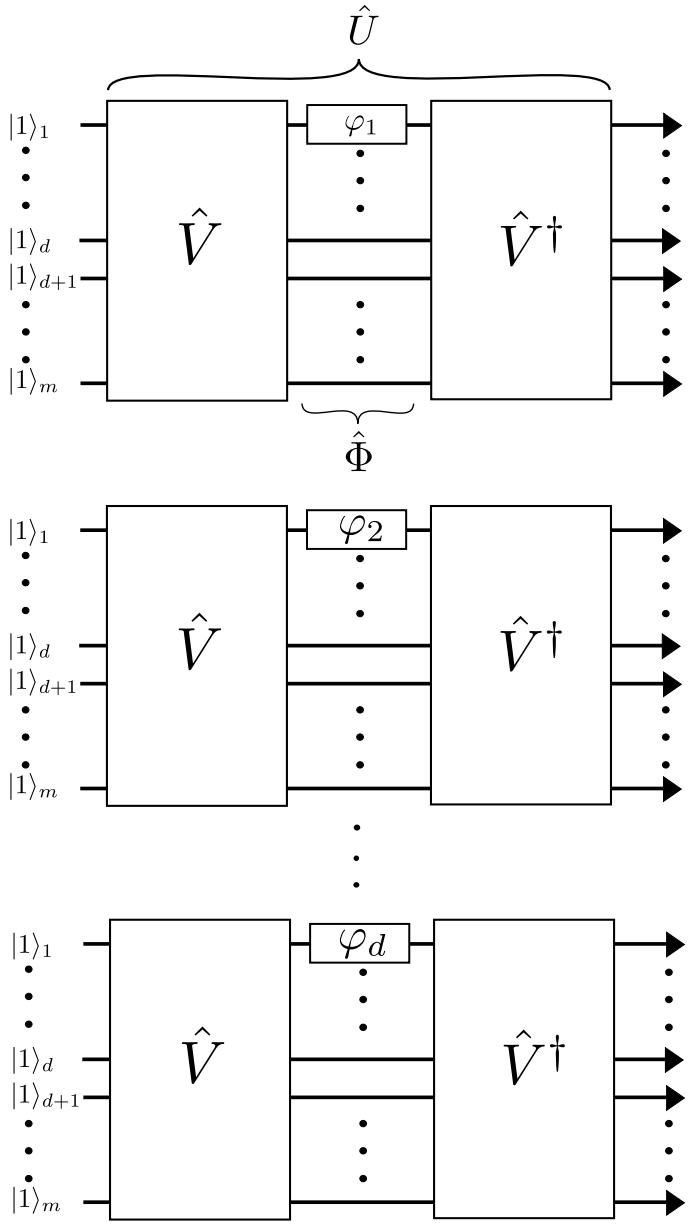

Figure G.1: Architecture of the sequential QUMI optical interferometer, which independently measures d independent unknown phases $\{\varphi_j\}_{j=1}^{d}$. The interferometer consists of m modes with an input of m single photons, $|1\rangle^{\otimes m}$. The unitary $\hat{V}$ (and its conjugate) is a quantum Fourier transform implemented with a network of beamsplitters and phase shifters. The phases are placed on the first mode of each QUMI optical interferometer for simplicity.

Vita

Chenglong You was born in Taiyuan, Shanxi Province, China, 1991. He attended Qingdao University and graduated with a bachelor of science in Optical Information Science and Technology in 2014. His thesis is about rigorous coupled-wave analysis for surface-relief gratings.

He joined the Department of Physics and Astronomy at Louisiana State University in 2014. He immediately joined the QST group under the supervision of Prof. Jonathan P. Dowling and Prof. Georgios Veronis. Since then he has been working on the theory of quantum metrology, quantum optics, and photonics. He was a visiting research scholar at New York University, Shanghai in summer of 2017 and worked with Prof. Tim Byrnes. In summer of 2018, he worked as a research intern at National Institute of Science and Technology in Tokyo, Japan under Dr. Masahiro Takeoka. He also visited Prof. Feihu Xu at University of Science and Technology of China (USTC) in summer of 2018.